SRI International

Final Report • September 1997

SMART OPTICAL MEMORY

Ravinder Kachru, Principal Investigator

SRI Project 5310
Contract No. F49620-93-C-0076
MP 97-110

Prepared for:

Air Force Office of Scientific Research
Directorate of Physics and Electronics
AFOSR/NA
110 Duncan Avenue, Suite B115
Bolling AFB, DC 20332-0001

Attention: Dr. Alan Craig

Approved by:

David R. Crosley, Director
Molecular Physics Laboratory

David M. Golden
Senior Vice President
Chemicals, Energy, and Materials Division

DTIC QUALITY INSPECTED A
Approved for public release;
Distribution Unlimited

AFOSR-TR-97

0535

REPORT DOCUMENTATION PAGE

Public reporting burden for this collection of information is estimated to average 1 hour per response, including the time for reviewing instructions, searching existing data sources, gathering and maintaining the data needed, and completing and reviewing the collection of information. Send comments regarding this burden estimate or any other aspect of this collection of information, including suggestions for reducing this burden, to Washington Headquarters Services, Directorate for information Operations and Reports, 1215 Jefferson Davis Highway, Suite 1204, Arlington, VA 22202-4302, and to the Office of Management and Budget, Paperwork Reduction Project (0704-0188), Washington, DC 20503.

1. AGENCY USE ONLY *(Leave blank)*	2. REPORT DATE	3. REPORT TYPE AND DATES COVERED
	970900	Final 30 Sep 93 - 31 Mar 97

4. TITLE AND SUBTITLE

Smart Optical Memory

5. FUNDING NUMBERS

61101E
A 269/05

6. AUTHOR(S)

Ravinder Kachru

7. PERFORMING ORGANIZATION NAME(S) AND ADDRESS(ES)

SRI International
333 Ravenswood Avenue
Menlo Park, CA 94025-3493

8. PERFORMING ORGANIZATION REPORT NUMBER

PYU-5310

9. SPONSORING/MONITORING AGENCY NAME(S) AND ADDRESS(ES)

Air Force Office of Scientific Research
Directorate of Physics and Electronics/AFOSR/NE
110 Duncan Avenue, Suite B115
Bolling AFB, DC 20332-0001

10. SPONSORING/MONITORING AGENCY REPORT NUMBER

F49620-93-C-0076

11. SUPPLEMENTARY NOTES

19971021 262

12a. DISTRIBUTION/AVAILABILITY STATEMENT

A APPROVED FOR PUBLIC RELEASE; DISTRIBUTION UNLIMITED

12b. DISTRIBUTION CODE

13. ABSTRACT *(Maximum 200 words)*

Sequential computers are fast approaching the fundamental physical limits of performance. Computers capable of parallel processing are being used to improve performance. These parallel computers or processors require fast, dense, affordable, intelligent main and cache memories. SRI International is developing a high density, random access, smart time-domain optical memory (TDOM) to meet the above needs. SRI performed experiments to examine the practicality of the photon echo approach to serial data storage. SRI successfully demonstrated a storage density of 2 Kbits in frequency channels 110 MHz wide in Eu doped Y_2SiO_5 crystal at an input/output speed of 40 MHz. No measurable cross-talk between adjacent frequency channels was observed. From these measurements, a memory density of 6.25×10^4 bits/focal spot was inferred, which is the highest storage density demonstrated to date. This work shows that this serial architecture for optical data storage is extremely valuable for applications such as all-optical switching.

DTIC QUALITY INSPECTED 4

SRI International also performed a feasibility study to examine the use of stimulated echo technique for parallel optical data storage. In a proof-of-principle experiment, a total of 100 single-page

14. SUBJECT TERMS			15. NUMBER OF PAGES
Optical memories	Optical data	Recording	
Digital holographic memory	Optical packet decoding	High speed memory	16. PRICE CODE
Optical cache memory			

17. SECURITY CLASSIFICATION OF REPORT	18. SECURITY CLASSIFICATION OF THIS PAGE	19. SECURITY CLASSIFICATION OF ABSTRACT	20. LIMITATION OF ABSTRACT
UNCLASSIFIED	UNCLASSIFIED	UNCLASSIFIED	Unlimited

CLASSIFIED BY:

N/A since Unclassified.

DECLASSIFY ON:
N/A since Unclassified.

13. ABSTRACT (Continued)

holograms were stored and later recalled successfully. The results suggest a frame transfer rate exceeding 10^3 frames per second along with a high storage density. The experimental results from this project clearly demonstrate the feasibility of the TDOM for high speed, high density, optical data storage application using existing technology.

SUMMARY

Sequential computers are fast approaching the fundamental physical limits of performance. Computers capable of parallel processing are being used to improve performance and to achieve the computation speed required for solving problems such as image analysis and image recognition. These parallel computers or processors require fast, dense, affordable, intelligent main and cache memories. A memory density of 10^{12} bits/cm^3, a data transfer speed of several gigabits per second, and a fast access time are often needed for applications, such as all-optical switching on fiber-optic networks. The projected extension of current memory technology cannot meet these requirements.

SRI International is developing a high density, random access, smart time-domain optical memory (TDOM) to meet the above needs. The Advanced Research Projects Agency, under the Ultra program, supported our work to demonstrate the potential of TDOM for high speed, high density, optical data storage.

During the past three years, SRI International investigated many issues related to the practical development of this high speed, high density, smart optical memory based on stimulated echo. Because most experiments performed on the TDOM concept have been at the proof-of-concept stage, a series of experimental studies that address the feasibility of the technology were performed. The primary objective was to find out the storage capacity of TDOM that, with a reasonable data rate, can be obtained using existing technology. In addition, miniaturization of TDOM and single-event detectability of the signal were also investigated. In this final report, the results are described.

SRI performed experiments to examine the practicality of the photon echo approach to serial data storage. SRI successfully demonstrated a storage density of 2 Kbits in frequency channels 110 MHz wide in Eu doped Y_2SiO_5 crystal at an input/output speed of 40 MHz. Using a simple photodiode, we faithfully retrieved the stored data with high signal to background ratio on a single event basis. No measurable cross-talk between adjacent frequency channels was observed. From these measurements, a memory density of 6.25×10^4 bits/focal spot was inferred, which is the highest storage density demonstrated to date. This work shows that this serial architecture for optical data storage is extremely valuable for applications such as all-optical switching.

SRI International also performed a feasibility study to examine the use of stimulated echo technique for parallel optical data storage. In a proof-of-principle experiment, a total of 100 single-page holograms were stored and later recalled successfully. The results suggest a frame transfer rate exceeding 10^3 frames per second along with a high storage density. The practical limits on storage capacity at a single spatial location were also examined. The projected capacity is 1000 images per spot. In addition, SRI developed and tested a demonstration system that permits data transfer at the video rate.

The experimental results from this project clearly demonstrate the feasibility of the TDOM for high speed, high density, optical data storage application using existing technology.

CONTENTS

FIGURES

INTRODUCTION

Sequential computers are fast approaching the fundamental physical limits of performance. Computers capable of parallel processing are being used to improve performance and to achieve the computation speed required for solving problems such as image analysis and image recognition. These parallel computers or processors require fast, dense, affordable, intelligent, main and cache memories. A memory density of 10^{12} bits/cm^3, a data transfer speed of several gigabits per second, and a fast access time are often needed for applications, such as all-optical switching on fiber-optic networks. The projected extension of current memory technology cannot meet these requirements.

SRI International is developing a high density, random access, smart time-domain optical memory (TDOM) to meet the above needs. The Advanced Research Projects Agency, under the Ultra program, supported our three-year project to demonstrate the potential of TDOM for high speed, high density, optical data storage.

Most of the previous work in time-domain data storage concentrated on making spectroscopic measurements of rare-earth doped materials to infer storage density and speed. The theoretically predicted density and speed for TDOM are 10^{12} bits/cm^3 and 10^{10} bits/s, respectively.

Determining the realistic limits that current technology and materials place on storage density, storage speed, and other critical parameters (such as compactness and signal-to-noise ratio) is an important task for the TDOM scheme and for other advanced optical memory schemes. Such studies provide useful information about the realistic performance that TDOM can deliver, and give direction to future research.

We demonstrated the intelligent feature of the TDOM by devising a novel scheme for high speed processing of optical header information. In this scheme, incoming headers are rapidly analyzed by performing simultaneous correlation operations with a large number of headers stored in advance through angular multiplexing. Decoding is accomplished by identifying the directions that yield the maximum correlation signal. We performed a proof-of-principle experiment in which two 5-byte ASCII addresses were decoded successfully. These results demonstrate that the prospect of using TDOM for optical packet switching is promising.

In this final report, we describe the experiments in which 2 Kbits long serial data was stored with good signal to noise ratio. From these experiments, a memory density of 6.25×10^4 bits/focal volume can be inferred.

In this report, we also summarized the result of a series of experiments in which two-dimensional images were stored. A total of 100 single-page holograms were stored. Our results show that a frame rate of 10^3/sec is feasible.

BACKGROUND

To illustrate the storage of information in the time domain using hole burning materials, we use a simple diagram to describe the storage and retrieval of, first, a single bit, and then several bits, of information. Figure 1(a) shows the temporal sequence of laser pulses (i.e., the write, data, and read pulses) required to store and retrieve several bits of serial information. The frequency of the laser excitation pulses is fixed to a particular color that is in resonance with a particular group of atoms within the larger absorption line of the memory crystal. We use a rare-earth ion doped in a crystal as our memory crystal. At low temperatures (4 to 10 K), the width of the frequency absorption of a single rare-earth ion is very small (a few kilohertz). However, the overall absorption width of the memory crystal is much larger (many gigahertz) because the rare-earth ions occupy different sites in a crystal. Therefore, individual ions do not see the write and data pulses that occur respectively at times $t_W = 0$ and t_D as two different pulses but rather as a complex pulse with a well-defined frequency Fourier transform (FT).

For simplicity, Figure 1(b) shows the frequency FT of the write pulse and one of the data pulses from Figure 1(a). The FT of the three-pulse data pulse train shown in Figure 1(a) will be more complex than that shown in Figure 1(b). Figure 1(b) shows that the excitation spectrum is not uniform but is amplitude-modulated at frequencies proportional to the FT of the data pulse train. Therefore, the absorption of the memory crystal around the color of the laser itself will be modulated as a function of the absorption frequency. In other words, within a micron-sized pixel in the memory crystal, the serial bits representing information in the time domain are stored by a small group of atoms absorbing a particular color of light by Fourier transforming the temporal signal into frequency-domain absorption modulation. The information can be stored for many hours at low temperatures in a Eu^{3+}:Y_2SiO_5 crystal.[1-3]

To read the information, we need only excite the memory crystal at time t_R with a single laser pulse of the same color as the data and write pulses. The read pulse causes the atoms to take the inverse Fourier transform of the frequency population modulation, and the result is a coherent emission or echo by the memory crystal at time $t_R + (t_D - t_W)$. The echo pulse emitted by the memory crystal mimics the data pulse train, and the serial data can therefore be retrieved. Furthermore, the coherent nature of the emitted signal from the memory crystal allows the entire signal to be captured by a single detector at a high signal-to-noise ratio.

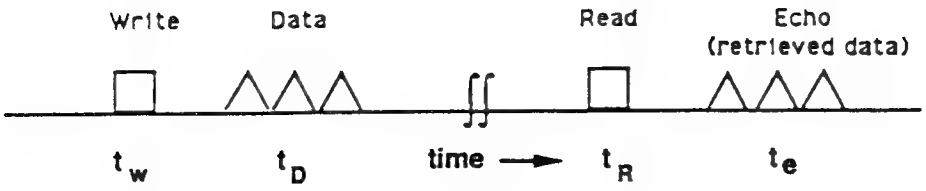

(a) Temporal sequence of laser pulses.

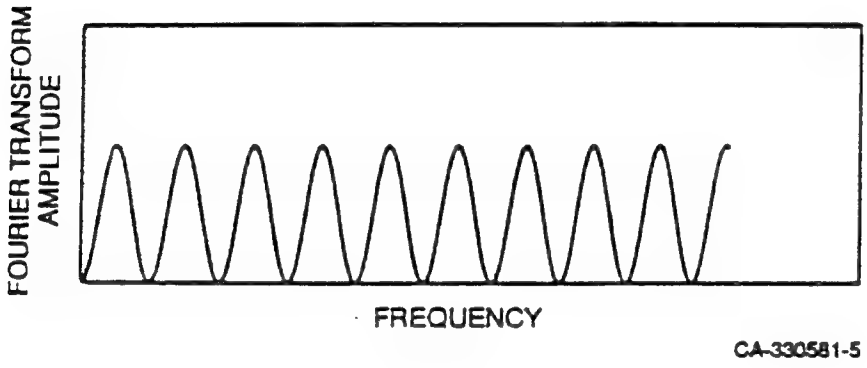

(b) Frequency Fourier transform of the write pulse and a single data pulse shown in (a)

Figure 1. Storage and retrieval of information.

We can begin to evaluate the potential storage density and read/write speeds for the stimulated echo (SE) memory approach by considering the restrictions placed on the laser pulses by the spectral properties of the absorbing atoms. The first requirement is that the laser pulses be separated by enough time that they are distinguishable. The minimum temporal separation between neighboring pulses is given by

$$\tau_p = \frac{1}{\pi \delta_I} \tag{1}$$

where δ_I (called the inhomogeneous linewidth) is the spread in the absorption frequencies of the atoms in the various sites in the sample.

The second requirement is that the last data pulse arrive while the excited atomic dipoles can still compare it with the first data pulse. The maximum time between the first and last data pulse is given by

$$T_2 = \frac{1}{\pi \delta_H} \tag{2}$$

where δ_H (called the homogeneous linewidth) is the effective absorption linewidth of an atom at a specific site. T_2 is also called the dephasing lifetime. Its maximum value is the radiative lifetime of the excited state.

Thus, T_2/τ_p (or equivalently δ_I/δ_H) bits of information can at most be stored in a single spot, and the read/write rate is just $1/\tau_p$. For Eu^{3+} doped in Y_2SiO_5 (the optimum storage material), the ratio δ_I/δ_H is 5×10^6 and $\tau_p = 100$ ps, resulting in a read/write rate of greater than 10^{10} bits/s and a storage density of more than 10^6 bits per spatial spot.

RESULTS

RANDOM ACCESS MEMORY

Stimulated echo memory, also called TDOM, is a high speed, dense optical memory and is intrinsically massively parallel. In the standard implementation of the SE memory, long word sizes in the range of 10^4 to 10^5 bits emerge in a natural way to achieve the high density optical storage. The long word size is reasonable and perhaps desirable for some random mass memory applications. However, in contrast, random-access memory application requires partitioning the memory into smaller subunits so that each memory location has the following features:

- Word size should be smaller (16, 32, 64, 128... bits long), so that each memory location is randomly accessible for both reading and writing without other locations being affected.
- The contents of each memory location should, in principle, be independently erasable.
- Reading and writing to different memory locations simultaneously should be possible.

To address these random-access memory features, we developed a new data storage scheme that is, in essence, a hybrid of the time-domain SE concept and the frequency-domain hole-burning scheme.[1-5] The new idea is to partition the absorption frequency domain into smaller bins, so that each frequency bin stores a smaller amount of information independently. The bins are distinguishable by their different absorption frequencies, and they are accessed by changing the laser frequency (color). However, information is still read and written using the SE concept (i.e., the time-domain pulse sequence).

TIME-FREQUENCY DOMAIN STORAGE

Because the SE memory can store 10^{12} bits/cm^3, its true potential can be realized by storing information not only in the time domain but also in the frequency domain of a single pixel in the memory crystal. For example, as shown in Figure 2, the entire absorption frequency of the memory crystal can be subdivided into N frequency bins (colors), each of which can store several bytes of serial information. This storage can be accomplished by using a narrow linewidth laser and setting its frequency (color) to the center of one bin. The pulse sequence

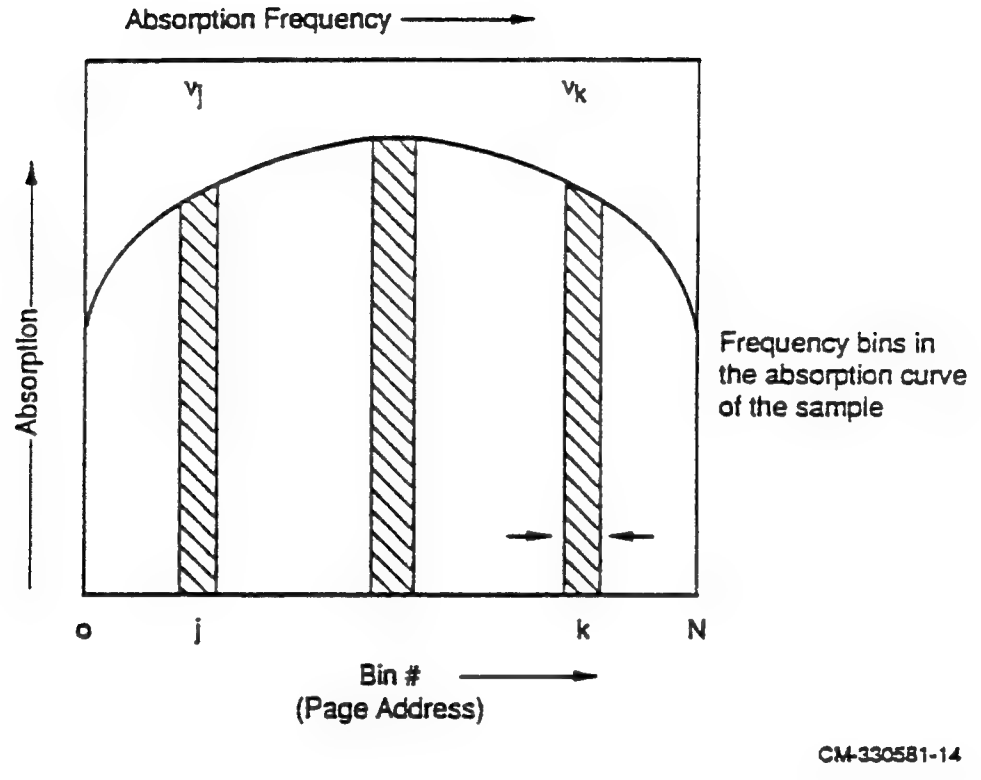

Figure 2. Division of absorption frequency spectrum into N frequency bins.

shown in Figure 1(a) now stores and retrieves the serial information at this frequency bin within a pixel.

SERIAL RANDOM ACCESS MEMORY USING A TIME-FREQUENCY APPROACH

The TDOM approach is well suited to storing digital information using a time serial approach. The serial approach is employed not only in digital computer storage environments (e.g., DRAM, magnetic media) but also in high speed fiber-optic communication infrastructures. All-optical switching of information carried on a fiber-optic backbone requires a bit serial optical memory. We expect the serial optical memory we are developing to have a major use as a memory device for future all-optical network switching.

As a first step toward developing a high speed serial memory, we demonstrated the potential of the time-frequency domain memory using a rare-earth doped crystal. These experiments were performed on the 579.88 nm transition ($^7F_0$-$^5D_0$, site 1) of a 0.1% Eu^{3+}:Y_2SiO_5 crystal[5,6] at 2 K. This transition has inhomogeneous broadening of 3.6 GHz and a homogeneous linewidth of 400 Hz, corresponding to a dephasing time of ~800 μs.

The optical pulse sequence was generated by acousto-optically modulating the cw dye laser with pulse 1 as the write pulse and pulse 2 as the data pulse, which is a binary-encoded pulse train with a rate of 40 Mbits/s.

At first, we successfully stored 45 bits of data in a single spatial spot.[7] When we tried to increase the storage beyond 50 bits, we were unsuccessful because of a phenomenon known as coherent saturation. Whenever a long pulse train (such as the data pulse) is created from a coherent source (such as a laser), its Fourier spectrum consists of a narrow zero-modulation frequency peak and equally narrow sidebands separated by the modulation frequency (40 MHz, in our case). Because the Fourier spectrum of the data pulse train is not evenly spread over the modulation bandwidth, absorption occurs in only a small fraction of ions whose absorption frequencies lie at the peaks of the FT, and a large fraction of the ions do not participate in the storage of information. Consequently, a saturation occurs, particularly at the zero modulation frequency.[1,2,8]

To avoid coherent saturation, we phase-modulated the data pulse by pseudorandom biphase shifting and by modulating the amplitude. The energy of the data was thus evenly distributed in the data bandwidth (80 MHz).

The echo signals were detected by an avalanche photodiode and recorded on a single-event basis by a digitizing oscilloscope. After each measurement, the laser was shifted by 110 MHz to a "fresh" spot. The power of the observed echo signal was about 0.01% that of the

input data pulse when t_{32} (storage time) was shorter than the excited state lifetime (2 ms). Echo signals with large t_{32} were about 30 times smaller.

Figure 3 shows the results of a typical experiment with collinearly propagated pulses. Figure 3(a) shows the input pulse sequence and the echo signal (retrieved data) for a 10 μs data pulse (400 bits). The input pulses are attenuated by ~10^{-4}. Figure 3(b) shows pulse 2 (input data) on an expanded time scale, and Figure 3(c) shows the retrieved data on an expanded time scale. Figure 3(d) shows the same data retrieved (with P_1 and P_2 off) after ~2 minutes. The signal was amplified by a factor of 26. No noticeable signal degradation was observed after reading was repeated up to ten times.[1,2]

Recently we increased the length of the data pulse to 2000 bits.[1] As mentioned earlier, the separation between the frequency channels used in this experiment was 110 MHz and the inhomogeneous width of the transition was 3.6 GHz. About 32 frequency channels should, in principle, be available on this transition. Thus, the storage capacity inferred from this experiment is $> 6.25 \times 10^4$ bits per spatial spot.[2] Taking into account the total excitation volume, we find that the storage density obtained here is 4×10^8 bits/cm^3.

In these experiments, the signal detectability was limited by the noise of our amplifier, which can be improved by a factor of 10. We can also increase the length of the crystal by a factor of 10. Taking this into account, we can improve the volume storage density to 0.8×10^{10} /cm^3, which sets the lower limit that can be obtained with existing technology.[11] The corresponding two-dimensional storage density is 2.4×10^{10} /cm^2, which is about three orders of magnitude higher than that of compact discs.

TIME-FREQUENCY DOMAIN HOLOGRAPHIC IMAGE STORAGE

Image storage in TDOM has been successfully demonstrated using high power pulsed lasers.[8-9] Like photochemical hole burning[10] and photorefractives,[11] this time-domain approach to image storage has the potential of offering ultrahigh storage density and fast data access time. Unlike other optical memories, TDOM can provide ultrahigh image transfer rates and offers features such as in-memory image processing.[12] However, difficulties arise in using the conventional time-domain approach to image storage, namely multiple images per frequency channel. For example, existing image composers such as electronically addressed spatial light modulator (SLM) do not have switching times fast enough to accommodate the required recording speeds ($\gtrsim$ MHz). High power pulsed lasers are needed to make retrieved images detectable by electronic cameras. In addition, features such as random frame (or page) access and variable playback speed are not available with the conventional approach.

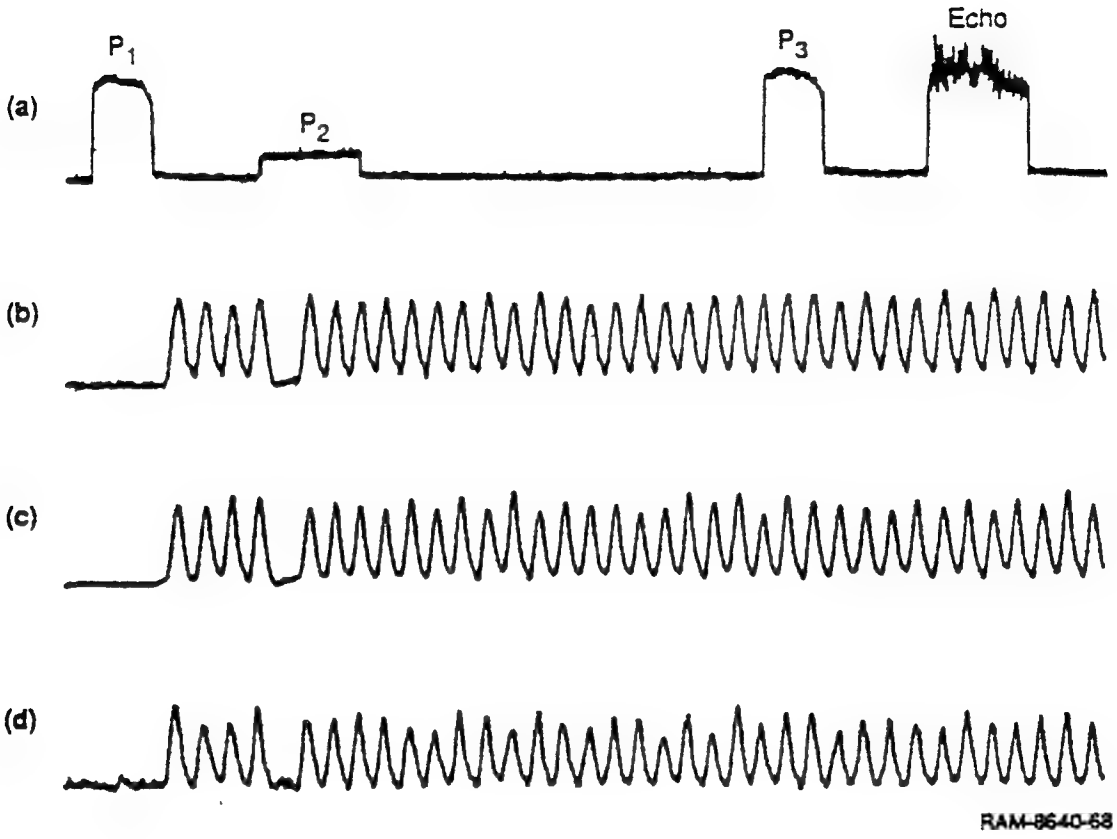

Figure 3. Results of a typical experiment with collinearly propagated pulses.

(a) Input pulse sequence and echo signal. Full horizontal scale = 102.4 μs. The duration of the data pulse is 10 μs (400 bits). The input pulses are attenuated by ~10^{-4}. (b) Input data pulse (P_2) on an expanded time scale. (c) Retrieved data pulse (echo) on an expanded time scale. (d) The same data retrieved (with P_1 and P_2 off) after ~2 minutes. The signal was amplified by a factor of 26.

We developed a new approach to time-domain image storage that not only retains those features that are unique to TDOM, but also permits random frame access and variable playback speed. Most importantly, it can be readily implemented with the use of existing low power cw lasers, a key requirement for a practical storage device.

In our approach, shown in Figure 4, two-dimensional input images are stored spectro-holographically in narrow ($\Delta\nu \leq 1$ MHz) frequency channels within an inhomogeneously broadened absorption line of a rare-earth solid by using a low-power cw laser, with one frame per frequency channel. Each image is stored by first tuning the laser wavelength to the desired channel and illuminating the sample with two temporally separated pulses known as the reference (E_{r_1}) and the object (E_o) pulses. E_{r_1}, a spatially uniform laser pulse carrying no information, precedes E_o, which carries the spatial information (e.g., an image) to be stored. E_o can be generated by transmitting a spatially uniform laser pulse through an SLM. The image thus recorded is a time-domain hologram resulting from the interference of the temporally delayed pulses via interaction with dipoles in the storage material.

The above recording procedure is repeated for subsequent input images at different channels. It can be initiated, for example, at the low frequency side of the inhomogeneous line and completed at the opposite side by incrementally increasing the laser wavelength at the corresponding input rate. For an inhomogeneous bandwidth of 4 GHz (typical of a rare-earth solid) and $\Delta\nu$ = 1 MHz, a total of 4000 images can be stored at one spatial location.

The image stored in a particular channel is recalled by tuning the laser wavelength to the channel location and exciting the sample with another reference pulse (or the read pulse, E_{r_2}), whose spatial profile is identical to that of E_{r_1}. The read pulse induces an echo that contains spatial information identical to E_o.[8,9]

The time required to record a single frame, τ_s, is determined by the temporal widths of E_{r_1}, E_o, and their separation. The separation can be limited to the width of the data channel to maximize the recording speed, e.g., for a wide data channel (1 MHz), the minimum separation can be as low as 1 μs. The channel switching time can be much shorter than τ_s for the small frequency increment proposed here (i.e., ≤ 1 MHz). Thus, the upper limit of the recording speed is determined mainly by the reciprocal of τ_s, and the reciprocal can be estimated from the efficiency of the echo pulse.

The temporal profile of an echo does not have to be identical to its input in the one-frame-per-channel approach. Thus, the requirements on E_{r_1} and E_{r_2} can be relaxed considerably to permit the use of long reference pulses for efficient echo conversions with a low power laser.

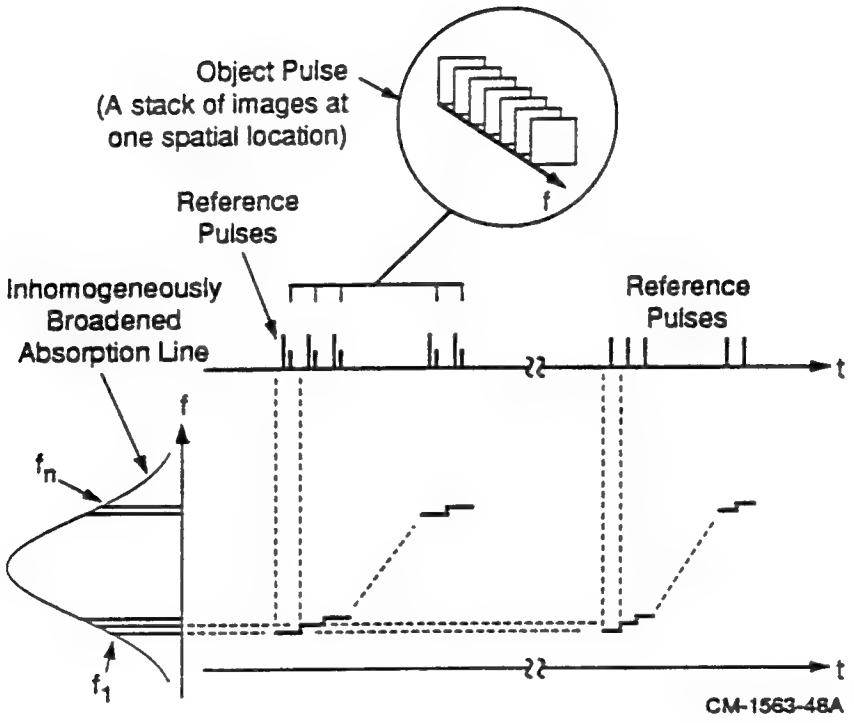

Figure 4. Schematic of the one-frame-per-channel approach to image storage in CTDOM.

The efficiency of three-pulse echoes is proportional to $\sin^2\theta_1 \sin^2\theta_2$ (here θ_i and θ_2 are the pulse areas of the first and second excitation pulses, respectively, with a maximum efficiency around 0.5%, i.e., when $\theta_1 = \theta_2 = \pi/2$.[9] In our experiments, the first and the second excitation pulses correspond to the reference and the object pulses, as shown in Figure 4. The efficiency is defined as the ratio of the echo intensity to the object beam intensity. For convenience, we assume that the laser used for image storage is a 500 mW, single-frequency, cw laser (commercially available) and that the images are reduced to approximately 1×1 mm before being stored in a CTDOM. Furthermore, the rare-earth electronic transitions used for image storage has a typical transition wavelength of 580 nm and an oscillator strength of $\sim 2 \times 10^{-8}$.

Under these conditions, the pulse area for a pulse 1 μs long is approximately equal to 1, giving rise to an echo efficiency of ~0.25%. If the object pulse is shorter than the reference pulses, the echo length is comparable to the length of the reference pulses. To a good approximation, we can use the latter to estimate the total number of photons in an echo to be $\sim 4 \times 10^9$ (assuming the object pulse power is also 500 mW). For a CCD camera consisting of 1000×1000 pixels, this gives an average intensity of ~4,000 photons per pixel, a signal level strong enough for faithful retrieval.

Unlike conventional time-domain storage, the one-frame-per-channel approach permits the playback speed to differ from the recording speed. The maximum playback speed is limited only by the length of E_{r_2} and, thus, can exceed the maximum recording speed, provided that the scattered light from read pulses in adjacent frequency channels does not interfere with the echo signal. Random frame access is now possible without further modification. Another advantage is that materials with short dephasing times ($\gtrsim \tau_s$) can be used here because of the short τ_s.

We experimentally demonstrated the use of our scheme for image storage in a Eu^{3+}:Y_2SiO_5 crystal (7 mm thick × 8 mm diameter and 0.1 atom %). The experiments were performed on the $^7F_0$-$^5D_0$ transition (site 1 at 579.88 nm) of the crystal at ~2.5 K. This transition has an inhomogeneous linewidth of ~4 GHz and its peak optical density for the sample is ~1.0. Figure 5 shows the experimental arrangement. The reference and object pulses, whose lengths were 14 and 4 μs respectively, were generated by modulating a cw ring laser (Coherent 699-29, with a linewidth of $\lesssim 0.5$ MHz) with two acousto-optic modulators. The object pulse was expanded to approximately 20 mm in diameter to illuminate masks for spatial encoding. The reference pulses were also expanded and collimated by a telescope, but only to ~2.5 mm. The peak power of the reference pulses (both E_{r_1} and E_{r_2}) was ~240 mW and that of the object pulse was ~190 mW. For experimental convenience, the separation between E_{r_1} and E_o was chosen to

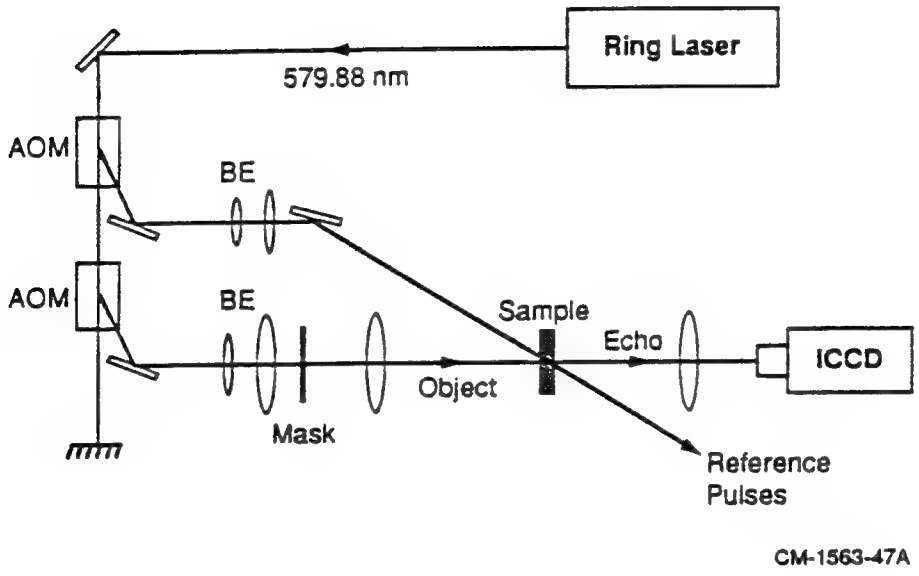

Figure 5. Experimental setup for time-domain holographic image storage. AOM, acousto-optic modulator; ICCD, intensified CCD camera; BE, beam expander.

be ~5 μs. Thus, τ_s is 24 μs, giving rise to a recording speed of ~4.1×10^4 frames per second (fps).

The arrangement of E_o and E_{r_1} (E_{r_2}) was similar to arrangements used in conventional holographic data storage, i.e., E_o and E_{r_1} (E_{r_2}) propagate along different directions and intersect at the sample as shown in Figure 5 (the intersecting angle was ~6°). Instead of imaging the input on the sample to the size required for efficient echo generation, we used a single lens and placed it behind the mask to focus the image down to approximately 1×1 mm. An identical lens was used behind the sample to reconstruct the focused image back to its original form, which was then detected by a gated, intensified, CCD camera (a 6×4.5 mm CCD chip with 610×488 pixels). The separation between the mask and focusing lens was equal to the focal length. The image stored was only an approximate Fourier image (because the sample was not exactly in the focal plane) and, as a result, its DC terms were spread over a much larger area (compared to an exact Fourier image) to prevent image-dependent saturation at the center.

This lens arrangement has several advantages. The spot size of E_o at the sample can be changed continuously by adjusting the input lens position to achieve optimum intensity. The recalled images are less affected by small defects in the storage materials, because any variation of material quality in the Fourier plane is distributed over the entire image upon inverse transformation. Furthermore, storing Fourier images gives the memory the ability to process the stored spatial information upon retrieval, a unique feature that has been demonstrated elsewhere.[11,12]

Four images generated by different black-and-white transparencies were stored into four separate data channels using our approach. The separation between two adjacent channels was 4 MHz. The stored information was later recalled by illuminating the sample with E_{r_2}. Figure 6 shows the results. The images were recalled 5 min after recording was completed, and they show no evidence of cross talk. In a separate experiment, the channel separation was reduced to 3 MHz and again no cross talk was detected. The results were obtained from single storage/ retrieval events with no signal averaging, and the echo efficiency was ~10^{-3}. The stored images can be recalled up to 20 times and the resulting echo images are still well within the detectable range of our recording system with no apparent degradation of image quality. Figure 7(a) shows such an example, which was obtained after repeated recall (14 times) from the same data channel (Channel 2).

We further examined the effect of long storage times on the fidelity of the recalled images, a vital issue in practical applications. Currently, such work can only be performed on a time scale of several hours because of the lack of laser stability beyond this time scale.

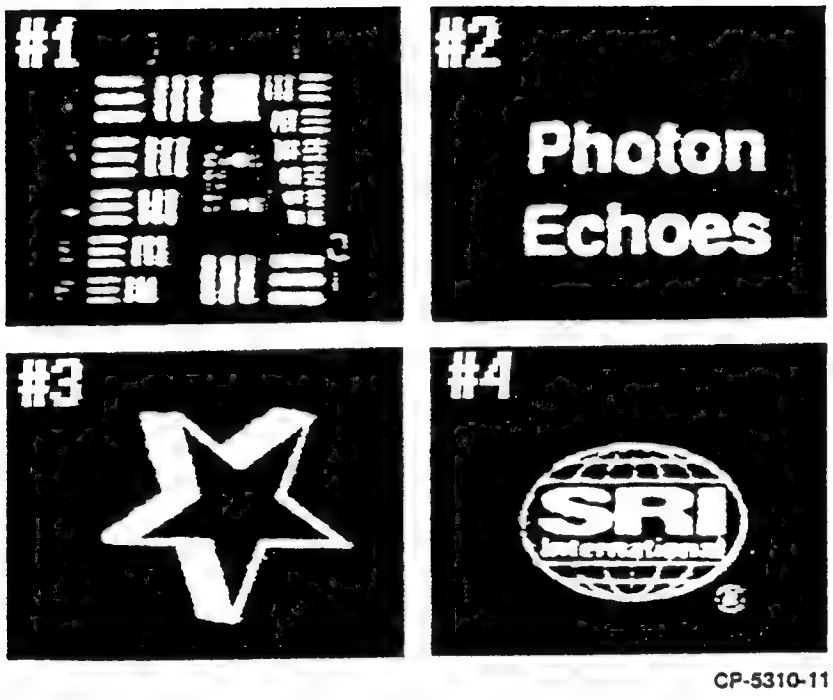

Figure 6. Experimental results demonstrating the storage of multiple images in CTDOM. The labels in the upper left corner of each image represent the data channel numbers. Each channel is 1 MHz wide and is separated from the next by 4 MHz. The images are recalled 5 min after recording is completed.

Figure 7. Echo images. (a) After repeated recall (14 times) from data channel 2. (b) Two hours after recording was compleed .

Figure 7(b) shows an image that was retrieved 2 h after recording was completed. Compared with Figure 6, it shows no noticeable change in echo efficiency and fidelity, suggesting that a storage time of several days or longer may well be possible with this storage material.

The quality of the recorded echo images was limited by the nonuniform response of the gated image intensifier in the CCD camera, which varied from shot to shot. We compared the images with their respective inputs detected by the same camera and found no measurable difference in image quality. We further recorded the same input images using a conventional CCD camera having no microchannel-plate intensifier and found a significant improvement in image quality. These findings suggest that the intrinsic quality of the images is much higher than what was observed. Another factor affecting the image quality is the Gaussian nature of laser spatial profiles. Spatially uniform laser beams are necessary for high quality image storage.

HIGH SPEED STORAGE OF WAVELENGTH-MULTIPLEXED VOLUME SPECTRAL HOLOGRAMS

We reviewed our scheme to store a large number of wavelength-multiplexed single-page spectral holograms in order to

- Examine the feasibility of using an SLM for information encoding in TDOM. This work is needed because of a large insertion loss introduced by an SLM.
- Determine the realistic limit on recording speed of an SLM-based TDOM.
- Examine the potential effect of wavelength multiplexing on diffraction efficiency as more holograms are stored. We successfully used wavelength multiplexing to record 100 spectral holograms at one spatial address in a $Eu^{3+}:Y_2SiO_5$ crystal. Despite the large insertion loss from the SLM, a frame recording speed in excess of 13 Kfps was obtained with a small laser power.

In TDOM, information is recorded in a storage medium as spectral interference patterns or spectral holograms.[6] Such interference is generated by exposing a spatial storage cell to two temporally separated laser pulses, referred to as the reference and data pulses. The data pulse carries the information to be stored through either spatial or temporal encoding. These two pulses resonantly excite the storage medium, generating a population grating in the ground state that is a replica of the spectral hologram. The hologram is thus stored.

To retrieve information, the population grating is illuminated with a read laser pulse identical to the reference pulse used in recording. Like conventional holography, this read pulse reconstructs the original data pulse through diffraction. However, the diffraction occurs in the time-domain rather than in the spatial domain, because the phase term in a spectral hologram

contains information about the temporal separation between reference and data pulses, not their spatial separation. Thus, the reconstructed pulse is temporally delayed with respect to the read pulse and is often known as stimulated photon echoes.[6]

Because spectral holograms are stored as population gratings, a transition with a large inhomogeneous linewidth is often desirable. More gratings can be recorded at the same spatial location by wavelength multiplexing to increase storage capacity. In our work, each spectral grating contains only one page of data (or one frame) generated by an SLM, thus offering random page access.

Our approach and the persistent spectral hole-burning (PSHB) approach to holographic recording differ fundamentally. In PSHB, the sample is exposed simultaneously to two laser beams and a simple featureless spectral hole is burned at the laser wavelength. The depth of the hole at a given location varies according to the spatial interference pattern generated by both beams. In TDOM, however, spatial interference is absent. A complex spectral grating (or hole pattern) is created only at locations exposed successively to both the reference and data pulses. Four-dimensional holograms, or volume spectral holograms, are recorded.

The experiments were performed on the $^7F_0$-$^5D_0$ transition (site 1 at 579.88 nm) of Eu^{3+}:Y_2SiO_5, which has an inhomogeneous linewidth of ~4 GHz and a dephasing time of ~1 ms. Figure 8 shows the experimental setup for storage and retrieval of volume spectral holograms. A computer entirely controlled recording and playback. In recording holograms, the computer first tuned to a desired wavelength (or data channel) within the inhomogeneously broaden absorption line, downloaded a preselected frame to an SLM through a frame grabber for information encoding, and then illuminated the sample with the reference and data pulses. This procedure was repeated at different channels until all 100 frames were stored. The data were later retrieved by illuminating each channel with a read pulse, and the reconstructed images were detected by a gated, intensified, CCD camera and digitized by the frame grabber.

The SLM used is a liquid crystal array taken from a projection television (InFocus TVT-6000). This array has 480 × 440 pixels and its insertion loss is approximately 97% for zero-order transmission. Two approaches can be used to compensate for the large loss: increase the laser power by a factor of 30 or increase the length of the data pulse because the camera detects time-integrated signals. The former approach is not practical because it would require a laser power of about 10 W. We chose the latter approach and used a data pulse 50 μs long with a peak power of only ~7 mW. The reference and read pulses were 14 μs long and biphase modulated with the 7-bit Barker code to obtain a data channel width of ~1 MHz. The separation between the

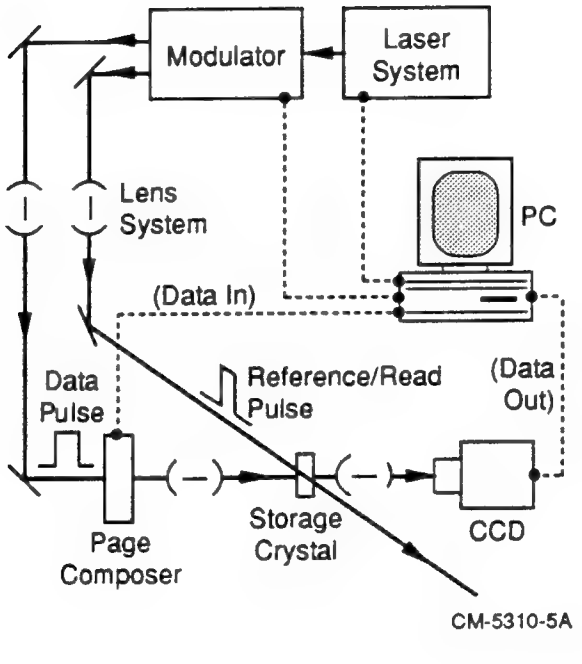

Figure 8. Experimental setup for demonstrating the use of an SLM to store 100 wavelength-multiplexed volume spectral holograms.

reference and data pulses was 10 μs, which in principle could be reduced to ~1 μs to increase the recording speed. The recording speed was 74 μs/frame, or 13.5 Kfps.

Five minutes after the recording was completed, we read out the data by illuminating each spectral grating with the read pulse. Figure 9 shows some of the reconstructed images. The 100 stored images were spaced evenly across a spectral window that was ~300 MHz wide and occupies only 7.5% of the inhomogeneous linewidth. Under this condition, we saw neither cross talk nor any effect on diffraction efficiency. A nearly constant efficiency of $\sim 10^{-3}$ was measured.

Because $^7F_0$-$^5D_0$ in Eu^{3+}:Y_2SiO_5[7] has two distinct optical sites, our experimental results suggest a minimum storage capacity of 2660 frames per spatial spot (or 1330 frames per optical site) for this one-frame-per-channel approach. We believe that by reducing the data channel width to ~0.5 MHz with a frequency-stabilized laser, a capacity of over 4000 frames per spatial spot is achievable in Eu^{3+}:Y_2SiO_5. We can further estimate this capacity for binary digital data storage. Assume that each page has 1000 × 1000 pixels and each information bit is represented by a block of 4 × 4 pixels. Under this condition, we would obtain a capacity in excess of 250 Mbits per spot. By taking into account the spot size (which is ~1.0 × 1.0 × 7.0 mm)[5], we would have a density of ~35 Gb/cm^3.

The above estimate can be further extended to the system's input/output bandwidth. For a page containing 250 × 250 bits, the achievable data throughput rate would exceed 840 Mbps. A more optimistic estimate that assumes one bit per pixel would yield a bandwidth of over 10 Gbps, which would be 100 times faster than the existing semiconductor cache memory.

OPTICAL HEADER ANALYSIS

Packet switching has emerged as a promising networking technique capable of supporting a wide range of communications services, such as voice, video, image, and data.[13,14] However, implementation of this technique at optical carrier frequencies for full use of the wide transmission bandwidth offered by fiber-optic technologies remains a challenge. One of the impediments to the development of this technique is its inability to permit rapid analysis of temporal optical information contained in the header of each packet for efficient routing. Most existing optical processors,[15,16] suffer from either insufficient memory capacity for storing reference information or slow processing speed for routing at required packet rates.

We demonstrated a novel scheme for rapid processing of temporal optical signals, such as optical headers. This scheme simultaneously uses three attractive features offered by the time-domain optical memory[17-24] (TDOM): the ability to perform in-memory temporal signal processing, high capacity for sequential data storage, and the ability to store reference signals

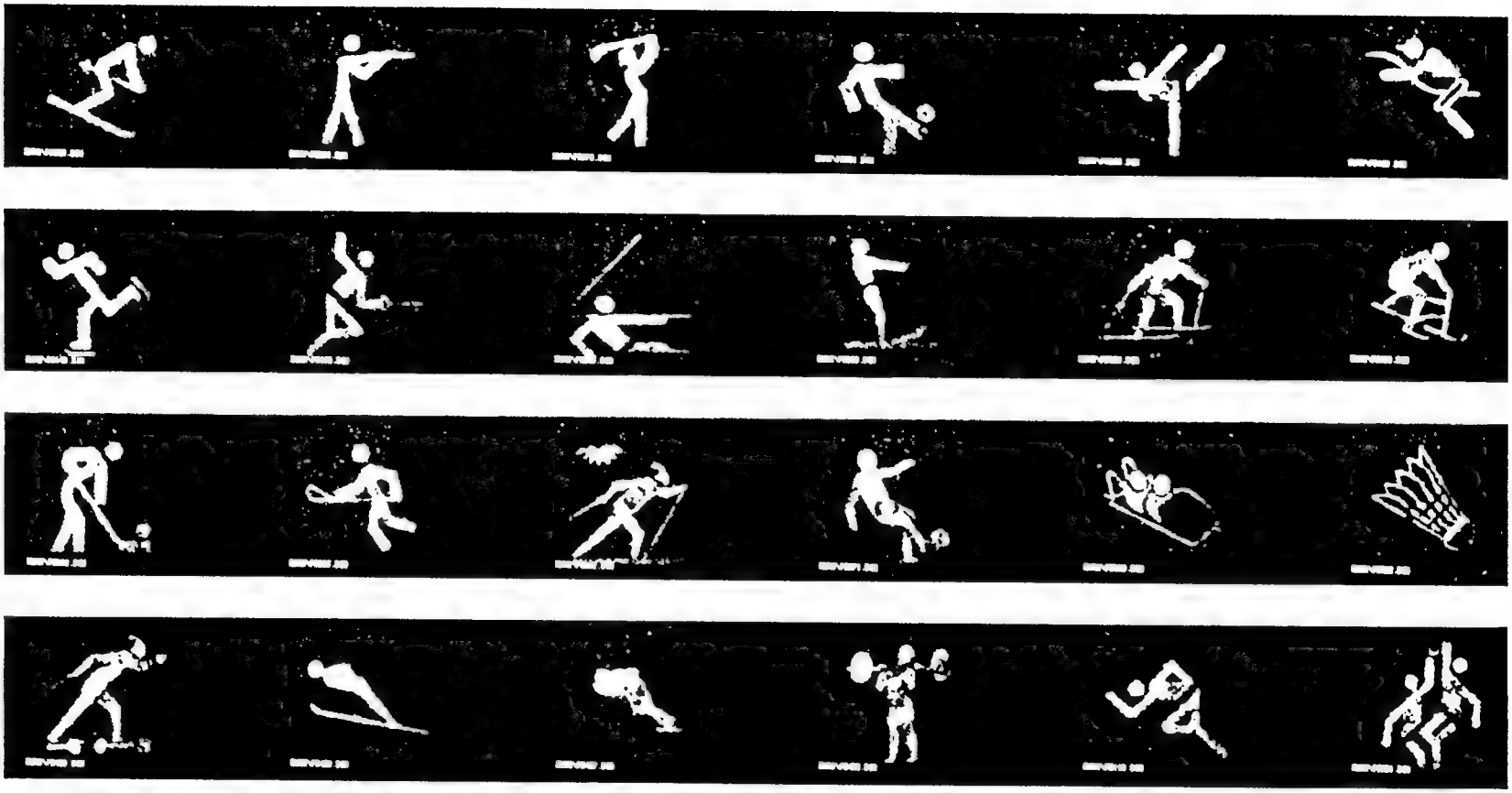

CPM-5310-18

Figure 9. Experimental results showing some of the reconstructed spectral holograms.

through angular multiplexing. Combination of these three features permits TDOM to simultaneously compare an incoming header and a large number of reference headers stored in advance through angular multiplexing for rapid parallel header processing, increasing significantly the processing speed.

Figure 10 illustrates the proposed scheme. In the programming phase, reference headers to be used for analysis are first stored through angular multiplexing at one spatial location by their respective brief write pulses. The reference headers (later the unknown headers to be analyzed) are chosen to propagate along a common direction $\hat{k}$ and are angularly multiplexed by variation of only the incident angle of the write pulses (e.g., the ith reference header H_i is stored by the ith write pulse W_i propagating along k_i). This process stores not only H_i for subsequent processing but also the propagation direction $\hat{k}_i$.

In TDOM, stored data are retrieved by use of a read pulse.[17] The pulse induces coherent radiation (often referred to as echoes) that mimics the temporal data sequence originally stored. Unlike other memory devices, data retrieved in TDOM is actually a process of temporal signal processing. In the case when a brief write pulse is used, the retrieved information represents either correlation or convolution of the read pulse with the stored data, depending on the order in which the write pulse is used.[18] With the choice of the pulse pair shown in Figure 10, the processing is simply a correlation operation, and the resulting echo is known to emit along the same direction as that of the write pulse. Thus, for the retrieved information to be identical to the stored information, a brief read pulse must be used. (Correlation of any function with a delta pulse yields the function itself.)

Parallel header decoding can now be realized as follows. If, instead of a brief read pulse, an unknown header H (propagating along $\hat{k}$) arrives at a sample at a later time, the echo generated along $\hat{k}_i$ is the correlation of H with H_i. A large correlation peak occurs when a match to H_i is found (i.e., $H = H_i$). Thus, one can identify H by examining the intensities of the correlation peaks along each direction. The advantage of monitoring correlation peaks is that decisions can be made very rapidly.

In a proof-of-concept experiment, we successfully used the proposed scheme to decode two 5-byte optical headers. For the purpose of demonstration, we chose the intensities of the two headers to represent the zip codes of SRI International and the Advanced Research Projects Agency in binary ASCII (i.e., 94025 and 22203, respectively). Details of the experimental apparatus are in Appendix D.

To generate two zip codes and their respetice write pulses, as shown in Figure 10, we employed three acousto-optic modulators and placed them in series in the beam pass, each of

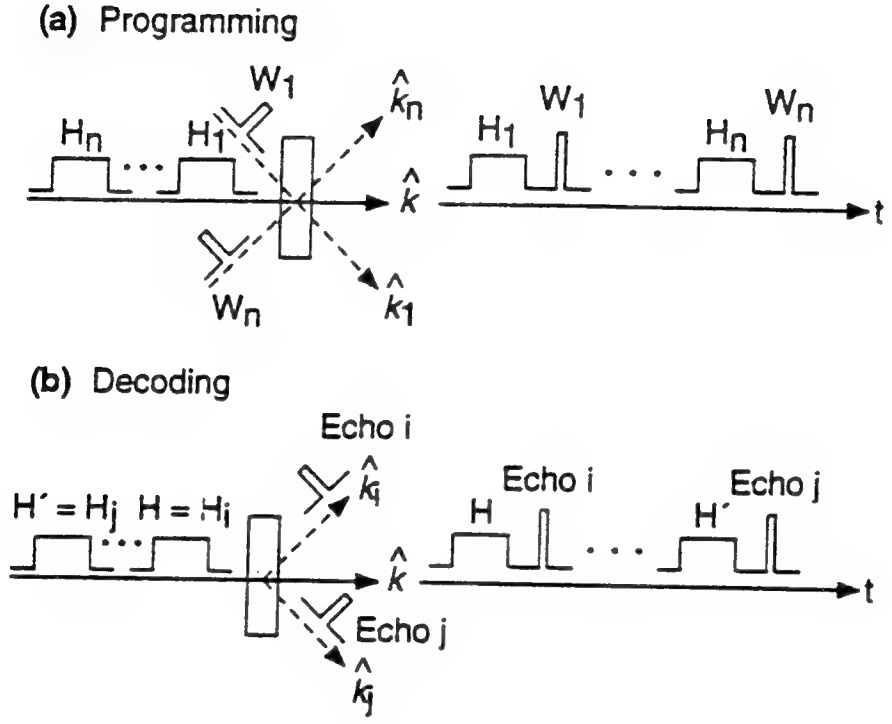

Figure 10: Schematic of the proposed scheme for optical header decoding. (a) The storage material is first programmed by exposure to n successive pulse pairs, each of which contains a reference header H_i and a write pulse W_i; each W_i is chosen to propagate along a different direction $\hat{k}_i$. (b) During the decoding, the sample is reexposed to unknown headers, and the echoes emitting in different directions are detected and compared.

which was used in a double-pass configuration. One acousto-optic modulator was responsible for generating two biphase-encoded zip codes, and the other two were responsible for generating two brief (~150-ns-long) write pulses in two separate directions.

Figure 11 shows the results. We first stored zip code 94025 by using a write pulse propagating along $\hat{k}_1$; 12 μs later, zip code 22203 was stored by another write pulse propagating along $\hat{k}_2$. Each "on" bit in the headers was represented by a 150-ns laser pulse, and the length of the headers was 12 μs. For experimental convenience, we chose the separation between the header and the write pulse in each pulse pair to be 12 μs. As discussed above, this separation can be reduced to 150 ns for the modulation used here.

After the completion of the header storage, we reexposed the sample first to zip code 94025 and then to zip code 22203 for decoding. The resulting correlation signals emitting in directions $\hat{k}_1$ and $\hat{k}_2$ were detected by two photodetectors. We chose the time between the completion of the memory programming and the start of the header decoding to be ~11 ms, much longer than the excited-state lifetime of the $^7F_0$-$^5D_0$ transition (i.e., 2 ms).[25] We know that the reference information used under such a condition in Eu^{3+}:Y_2SiO_5 can persist for hours or longer.[23-25]

Box 1 in Figure 11 shows the correlation signal along $\hat{k}_1$ and $\hat{k}_2$ after the arrival of zip code 94025. We obtained a strong correlation peak along $\hat{k}_1$ and no measurable peak along $\hat{k}_2$, indicating a good match to zip code 94025 and no match to zip code 22203. After the arrival of zip code 22203 (i.e., 24 μs later), the situation is reversed (see box 2 in Figure 11). No match was found along $\hat{k}_1$, whereas a good match was found along $\hat{k}_2$. As expected, the detected sharp peaks occurred exactly 12 μs after the arrival of each zip code (recall that the separation between H_i and W_i is 12 μs). Here, each correlation trace is 20 μs long and was recorded from a single processing event with no signal averaging.

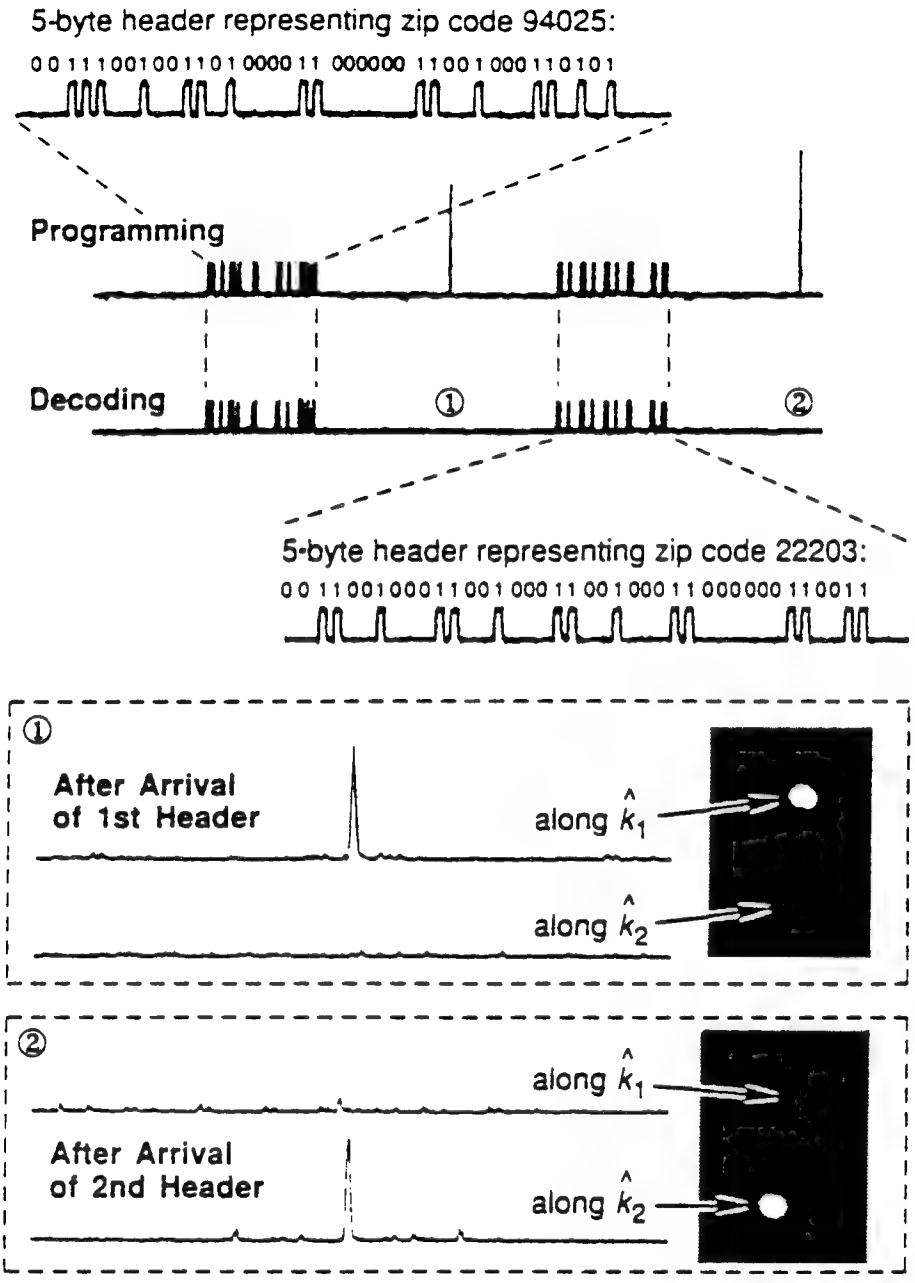

Figure 11: Experimental results showing the successful decoding of two zip codes. The second and third traces from the top display the input pulse sequence; the first and fourth traces are the two input zip codes on an expanded time scale. The recorded correlation signals along $\hat{k}_1$ and $\hat{k}_2$ after the arrival of zip code 94025 and zip code 22203 are shown in boxes 1 and 2, respectively.

CONCLUSIONS AND RECOMMENDATIONS

In conclusion, we have demonstrated the practical viability of 0 time domain optical memory both in the bit serial and bit parallel format. The inferred storage capacity of 6.25×10^4 bits per spatial spot, approaches the theoretical estimates. In addition, with frames rates of 10^3 frames/s, a high bandwidth parallel memory with applications to large server based memory device are feasible.

REFERENCES

1. R. Kachru, Y. S. Bai, and X. A. Shen, Advanced Materials **6**, 791 (1994). (Appendix A)

2. Y. S. Bai and R. Kachru, Opt. Lett. **14**, 1189 (1993).

3. X. A. Shen, E. Chiang, and R. Kachru, Opt. Lett. **19**, 1246 (1994). (Appendix B)

4. X. A. Shen and R. Kachru, Opt. Lett., to be submitted (Appendix C).

5. M. Mitsunaga, R. Yano, and N. Uesugi, Opt. Lett. **16**, 1890 (1991).

6. R. Yano, M. Mitsunaga, and N. Uesugi, Opt. Lett. **16**, 1884 (1991).

7. S. Kröll, L. E. Jusinski, and R. Kachru, Opt. Lett. **16**, 517 (1991).

8. N. W. Carlson, W. R. Babbitt, and T. W. Mossberg, Opt. Lett. **8**, 623 (1983).

9. M. K. Kim and R. Kachru, J. Opt. Soc. Am. B **4**, 305 (1987); M. K. Kim and R. Kachru, Opt. Lett. **12**, 593 (1987).

10. B. Kohler, S. Bernet, A. Renn, and U. P. Wild, in *Technical Digest on Persistent Spectral Hole-Burning: Science and Applications*, 1991 (Opt. Soc. Am., Washington, DC, 1991) Vol. 16, pp. 46-49; B. Kohler, S. Bernet, A. Renn, and U. P. Wild, Opt. Lett. **18**, 2144 (1993).

11. F. H. Mok, M. C. Tackitt, and H. M. Stoll, Opt. Lett. **16**, 605 (1991); F. H. Mok, Opt. Lett. **18**, 915 (1993).

12. E.Y. Xu, S. Kröll, D. L. Huestis, R. Kachru, and M. K. Kim, Opt. Lett. **15**, 562 (1990); X. A. Shen and R. Kachru, Opt. Lett. **17**, 520 (1992).

13. F. A. Tobagi, IEEE **78**, 133 (1990).

14. T. F. La Porta, M. Veeraraghaven, E. Ayanoglu, M. Karol, and R. D. Gitlin, IEEE Commun. Mag. (October 1994), p. 84, and references therein.

15. K. P. Jackson and H. J. Shaw, in *Optical Signal Processing*, J. L. Horner, ed. (Academic, New York, 1987), and references therein.

16. N. J. Bers, J. L. Lee, M. W. Casseday, and B. J. Udelson, Appl. Opt. **18**, 2767 (1979), and references therein.

17. T. W. Mossberg, Opt. Lett. **7**, 77 (1982).

18. Y. S. Bai, W. R. Babbitt, N. W. Carlson, and T. W. Mossberg, Appl. Phys. Lett. **45**, 714 (1984); Y. S. Bai, W. R. Babbitt, and T. W. Mossberg, Opt. Lett. **11**, 724 (1986).

19. Y. S. Bai and R. Kachru, U.S. Patent 5,369,665 (November 29, 1994).

20. M. Mitsunaga, R. Yano, and N. Uesugi, Opt. Lett. **16**, 1890 (1991).

21. R. Yano, M. Mitsunaga, and N. Uesugi, Opt. Lett. **16**, 1884 (1991).

Appendix A

TIME-FREQUENCY DOMAIN OPTICAL STORAGE IN RARE-EARTH DOPED MATERIALS

ADVANCED MATERIALS

Research News

Time-Frequency Domain Optical Storage in Rare-Earth-Doped Materials**

By Ravinder Kachru,* Yu Sheng Bai, and Xiao-An Shen

1. Introduction

Rare-earth-doped crystals were studied extensively in the 1960s and 70s as candidates for solid-state lasers. The best known of these crystals is neodymium doped in yttrium aluminum garnet (YAG). Over the last few years, there has been a resurgence of interest in these materials because of their interesting nonlinear optical properties.

At low temperatures, the intrinsic absorption linewidth of the ions, the homogeneous linewidth G_n, is about a kilohertz, the narrowest optical linewidth in a solid. The overall absorption width is considerably broader (typically a few GHz), however, because the rare-earth ions occupy a distribution of different sites in a crystal. The ratio of inhomogeneous to homogeneous width, a parameter which directly reflects the number of bits of information that can be stored in a single micrometer-sized spatial pixel, is approximately 10^6 in Eu:Y_2SiO_5 crystal. Furthermore, by using the time-domain technique, also known as stimulated echo, serial read/write data rates of 100 MHz have been obtained using this crystal. Applications of the time-domain approach[1-5] using rare-earth-doped crystals include high-speed memory, signal processing,[6] high-speed optical switching, optical interconnects image processing,[7] and logic operations.[8]

2. Optical Linewidths at Low Temperatures

The lanthanide rare-earth series is characterized by 4f valence electrons and a filled Xe core. Because of the incomplete shielding by the Xe core electrons, the f electrons tend to contract so that the main peak lies inside the Xe core. As a result, the rare-earth ions interact weakly with surrounding crystal fields and retain many of the free ion properties. At low temperatures, the phonon broadening of the optical line becomes negligible, and a very narrow linewidth approaching a few hundred hertz is observed.

[*] Dr. R. Kachru, Dr. Y. S. Bai, Dr. X.-A. Shen
Molecular Physics Laboratory, SRI International
333 Ravenswood Avenue, Menlo Park, CA 94025 (USA)

[**] This research was supported by the Advanced Research Projects Agency of the US Department of Defense, under Contract No. F49620-93-C-0076.

3. Time-Domain Memory

To illustrate the storage of information in the time domain by use of hole-burning materials, we use a simple diagram to describe the storage and retrieval of first a single bit, and then several bits, of information. Figure 1a shows the temporal sequence of laser pulses (the write, data, and read pulses) required to store and retrieve several bits of serial information. The frequency of the laser-excitation pulses is in resonance with a specific group of atoms within the larger absorption line of the memory crystal. At low temperatures (4 to 10 K), the width of the frequency absorption of a single rare-earth ion is very small (a few kilohertz). However, the overall absorption width of the memory crystal is much larger (many gigahertz) because the rare-earth ions occupy a distribution of different sites in a crystal. Therefore, individual ions see the write and data pulses occurring, respectively, at times $t_w = 0$ and t_D not as two different pulses but rather as a complex pulse with a well-defined frequency Fourier transform.

For simplicity, Figure 1b shows the frequency Fourier transform (FT) of the write pulse and one of the data pulses from Figure 1a. The periodicity of the FT shown in Figure 1b is proportional to $(t_D - t_w)^{-1}$. The FT of the three-pulse data-pulse train shown in Figure 1a will be more complex than that shown in Figure 1b. Figure 1b shows that the excitation spectrum is amplitude-modulated at frequencies proportional to the FT of the data pulse train.

Therefore, the absorption of the memory crystal near the center frequency of the laser will be modulated as a function of the absorption frequency. In other words, within a micron-sized pixel in the memory crystal, the serial bits representing information in the time domain are stored by a small group of atoms absorbing a particular color of light by Fourier transforming the temporal signal into frequency-domain absorption modulation. This absorption modulation can persist for many hours at low temperatures.[1-5]

To read the information, the crystal is excited by a single read pulse. The read pulse causes the atoms to take the inverse Fourier transform of the frequency population modulation, and the result is a coherent emission or stimulated echo (SE) by the memory crystal at time $t_R + (t_D - t_w)$. Under certain conditions, the echo pulse emitted by the memory crystal mimics the data pulse train, and the serial data can

 © VCH Verlagsgesellschaft mbH, D-69469 Weinheim, 1994 0935-9648/94/1010-0791 $5.00+.25/0

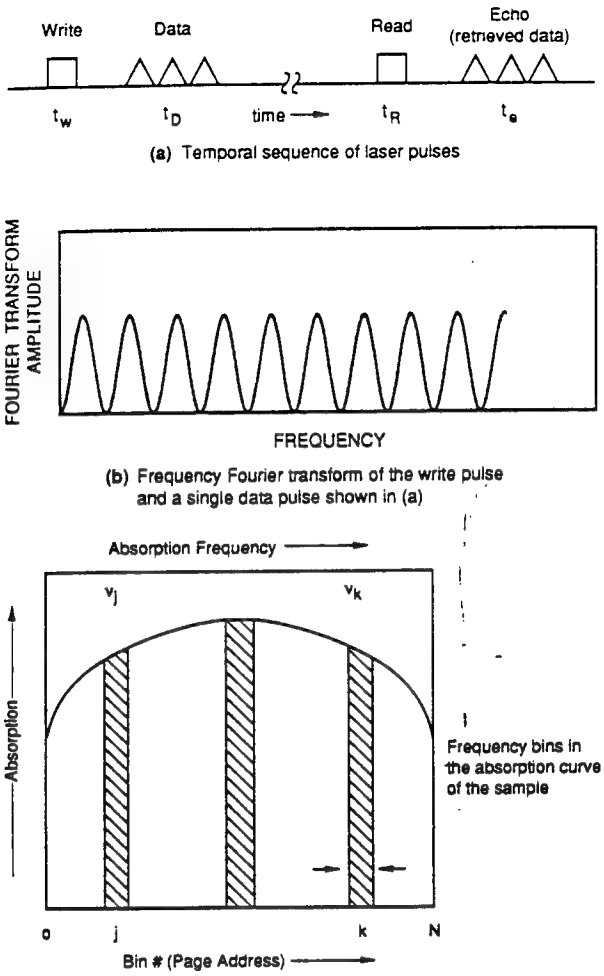

(a) Temporal sequence of laser pulses

(b) Frequency Fourier transform of the write pulse and a single data pulse shown in (a)

(c). Division of overall absorption frequency spectrum into N frequency bins.

Fig. 1. Storage and retrieval of information by the time domain technique. a) Temporal sequence of laser pulses. b) Frequency Fourier transform of the write pulse and a single data pulse shown in (a). c) Division of overall absorption frequency spectrum into N frequency bins.

therefore be retrieved. Furthermore, the coherent nature of the emitted signal from the memory crystal allows the entire signal to be captured by a single detector at a high signal-to-noise ratio.

The potential storage density and read/write speeds for the stimulated echo memory can be evaluated by considering the restrictions placed on the laser pulses by the spectral properties of the absorbing atoms. The first requirement is that the laser pulses be separated by enough time that they are distinguishable. The minimum temporal separation between neighboring pulses is given by $t_p = (1/\pi\delta_I)$, where δ_I (called the inhomogeneous linewidth) is the spread in the absorption frequencies of the atoms in the various sites in the sample.

The second requirement is that the last data pulse must arrive while the excited atomic dipoles can still compare it with the first data pulse. The maximum time between the first and last data pulse is given by $T_2 = 1/(\pi\delta_H)$ where δ_H (called the homogeneous linewidth) is twice the effective absorption linewidth of an atom at a specific site. T_2 is also called the dephasing lifetime. Its maximum value is the radiative lifetime of the excited state.

Thus, T_2/t_p (or equivalently, δ_I/δ_H) bits of information at most can be stored in a single spot, and the read/write rate is just $1/t_p$. For $Eu^{3\oplus}$ doped in Y_2SiO_5, the ratio δ_I/δ_H is 5×10^6 and $\tau_p = 100$ ps, resulting in a read/write rate of greater than 10^{10} bits/s and a storage density of more than 10^6 bits per spatial spot. Calculations show that up to 10^{12} bits/cm^3 can be stored volumetrically in rare-earth-doped crystals.

4. Time-Frequency-Domain Storage

Because the SE memory can store 10^{12} bits/cm^3, its true potential can be realized by storing information not only in the time domain but also in the frequency domain of a single pixel in the memory crystal. For example, as shown in Figure 1c, the entire absorption frequency of the memory crystal can be subdivided into N frequency bins (colors), each of which can store several bytes of serial information. This storage can be accomplished by using a narrow linewidth laser and setting its frequency (color) to the center of one bin. The pulse sequence shown in Figure 1a now stores and retrieves the serial information at this frequency bin within a pixel.

5. Practical Demonstration

To demonstrate the potential of the time-frequency domain memory using rare-earth-doped crystals, experiments have been performed on the 579.88 nm transition ($^7F_0 - {}^5D_0$, site 1) of a 0.1% $Eu^{3\oplus}:Y_2SiO_5$ crystal[9] at 2 K. This transition has inhomogeneous broadening of 3.6 GHz and a homogeneous linewidth of 400 Hz, corresponding to a dephasing time of ~ 800 μs.

The optical pulse sequence was generated by acousto-optically modulating the continuous-wave (cw) dye laser with pulse 1(3) as the write (read) pulse and pulse 2 the data, which is a binary-encoded pulse train with a rate of 40 Mbits/s.

Initially 45 bits of data were stored in a single spatial spot.[10] When we tried to increase the storage beyond 50 bits, we were unsuccessful. The reason for this failure was a phenomenon known as coherent saturation. Whenever a long pulse train (such as the data pulse) is created from a coherent source such as a laser, its Fourier spectrum consists of a narrow zero-modulation frequency peak and equally narrow sidebands separated by the modulation frequency (40 MHz, in our case). Because the Fourier spectrum of the data pulse train is not evenly spread over the modulation bandwidth, absorption occurs in only a small fraction of ions whose absorption frequencies lie at the peaks of the FT, and a large fraction of the ions do not participate in the storage of the information. Consequently, there is a saturation, particularly at the zero modulation frequency.[11]

© VCH Verlagsgesellschaft mbH, D-69469 Weinheim, 1994
0935-9648/94/1010-0792 $ 5.00+.25/0 Adv. Mater. 1994, 6, No. 10

To avoid coherent saturation, the data pulse was phase-modulated by pseudorandom biphase shifting in addition to the amplitude modulation. The energy of the data was thus evenly distributed in the data bandwidth (80 MHz).

The echo signals were detected by an avalanche photodiode and recorded on a single-event basis by a digitizing oscilloscope. After each measurement, the laser was shifted by 110 MHz to a "fresh" spot. The power of the observed echo signal was about 0.01 % that of the input data pulse when t_{32} (storage time) was shorter than the excited state lifetime (2 ms). Echo signals with large t_{32} were about 30 times smaller.

The results of a typical experiment with collinearly propagated pulses are shown in Figure 2. Figure 2a shows the input pulse sequence and the echo signal (retrieved data) for a 10 μs data pulse (400 bits). The input pulses are attenuated by $\sim 10^{-4}$. Figure 2b shows pulse 2 (input data) on an expanded time scale, and Figure 2c shows the retrieved data on an expanded time scale. Figure 2d shows the same data retrieved (with P_1 and P_2 off) after ~2 minutes. The signal was amplified by a factor of 26. No noticeable signal degradation was observed after reading was repeated up to 10 times.[11]

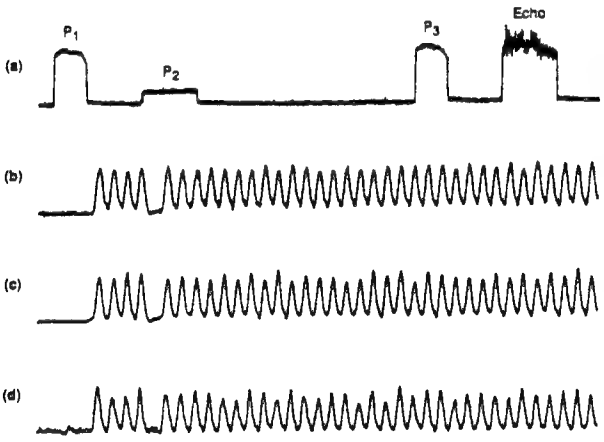

Fig. 2. Results of a typical experiment with collinearly propagated pulses. a) Input pulse sequence and echo signal. Full horizontal scale = 102.4 μs. The duration of the data pulse is 10 μs (400 bits). The input pulses are attenuated by $\sim 10^{-4}$. b) Input data pulse (P_2) on an expanded time scale. Full horizontal scale = 2.4 μs. c) Retrieved data pulse (echo) on an expanded time scale. d) The same data retrieved (with P_1 and P_2 off) after ~2 minutes. The signal was amplified by a factor of 26.

Recently, we have increased the length of the data pulse to 2000 bits. As mentioned earlier, the separation between the frequency channels used in this experiment was 110 MHz and the inhomogeneous width of the transition was 3.6 GHz. About 32 frequency channels should, in principle, be available on this transition. Thus, the storage capacity inferred from this experiment is $>6.25 \times 10^4$ bits per spatial spot. Taking into account the total excitation volume, we find that the storage density obtained here is 4×10^8 bits cm^3.

In these experiments, the signal detectability was limited by the noise of our amplifier, which can be improved by a factor of 10. Taking into account these factors, we can improve the volume storage density to 0.8×10^{10} cm^{-3}, which sets the lower limit that can be obtained with existing technology. The corresponding two-dimensional storage density is 2.4×10^{10} cm^{-2}, which is about 3 orders of magnitude higher than that of compact discs.

One of the inherent advantages of the time-frequency domain memory over electronic and magnetic memories is its ability to read and write information in parallel. The data rate can be substantially increased if the data pulses shown in Figure 1a carry spatial information, namely, two-dimensional images. Figure 3 shows one such image retrieved from a Eu:Y_2SiO_5 crystal. The image shown in Figure 3 was retrieved after being stored for 2 hours. Because the write, data, and read pulses used to store and retrieve the image shown in Figure 3 are approximately 5 μs long, we estimate that data in the two-dimensional frame format, with each frame having 10^6 pixels, can be stored and retrieved at 4×10^4 frames/s, which corresponds to a data rate of 40 Gbits/s.

Fig. 3. Image retrieved after 2 hours of storage.

[1] T. W. Mossberg, A. Flusberg, R. Kachru, S. R. Hartmann, *Phys. Rev. Lett.* **1979**, *42*, 1665.
[2] R. Kachru, T. W. Mossberg, S. R. Hartmann, *Opt. Commun.* **1979**, *30*, 57.
[3] T. W. Mossberg, *Opt. Lett.* **1982**, *7*, 77.
[4] N. W. Carlson, W. R. Babbitt, T. W. Mossberg, *Opt. Lett.* **1983**, *8*, 623.
[5] M. K. Kim, R. Kachru, *J. Opt. Soc. Am.* **1987**, *134*, 305.
[6] X. A. Shen, Y. S. Bai, R. Kachru, *Opt. Lett.* **1992**, *17*, 1079.
[7] X. A. Shen, R. Kachru, *Opt. Lett.* **1992**, *17*, 520.
[8] S. Kröll, U. Elman, *Opt. Lett.* **1993**, *18*, 1834.
[9] R. Yano, M. Mitsunaga, N. Uesugi, *Opt. Lett.* **1991**, *16*, 1884. M. Mitsunaga, R. Yano, N. Uesugi, *Opt. Lett* **1991**, *16*, 1890.
[10] S. Kröll, L. E. Jusinski, R. Kachru, *Opt. Lett.* **1991**, *16*, 51[illegible].
[11] Y. S. Bai, R. Kachru, *Opt. Lett* **1993**, *14*, 1189.

Appendix B

TIME-DOMAIN HOLOGRAPHIC IMAGE STORAGE

Time-domain holographic image storage

X. A. Shen, E. Chiang,* and R. Kachru

Molecular Physics Laboratory, SRI Laboratory, SRI International, Menlo Park, California 94025

Received April 5, 1994

We describe a practical approach to image storage in a coherent time-domain optical memory that can be readily implemented with existing technologies. In this approach, two-dimensional images are stored spectroholographically in narrow (≤1-MHz) frequency channels of a time-domain storage material by use of a low-power laser, with one image per channel. Advantages of this approach include fast single-frame recording time, variable playback speeds, and random frame access. Experimental results demonstrating the use of this approach for high-speed, long-term image storage in Eu^{3+}:Y_2SiO_5 are presented.

Image storage in coherent time-domain optical memory (CTDOM) has been demonstrated successfully by use of high-power pulsed lasers.[1,2] Like photochemical hole burning[3] and photorefractives,[4] this time-domain approach to image storage has the potential of offering ultrahigh storage density and fast data access time. Unlike other optical memories, CTDOM is capable of providing ultrahigh image transfer rates and offers features such as in-memory image processing.[5] However, difficulties arise in using the conventional time-domain approach to image storage, namely, multiple images per frequency channel. For example, existing image composers, such as electronically addressed spatial light modulators, do not have switching times (a megahertz or greater) fast enough to accommodate the required recording speeds. High-power pulsed lasers are needed to make retrieved images detectable by electronic cameras. In addition, features such as random frame (or page) access and variable playback speed are not available with the conventional approach.

Here we propose a new approach to time-domain image storage. This approach not only retains those features that are unique to CTDOM but also permits random frame access and variable playback speed. Most importantly, it can be readily implemented with the use of existing low-power cw lasers, a key requirement for a practical storage device.

In the proposed approach, two-dimensional input images are stored spectroholographically in narrow ($\Delta\nu \leq 1$ MHz) frequency channels within an inhomogeneously broadened absorption line of a rare-earth solid by using a low-power cw laser, with one frame per frequency channel (Fig. 1). One stores each image by first tuning the laser wavelength to the desired channel and illuminating the sample with two temporally separated pulses known as the reference (E_{r_1}) and the object (E_o) pulses. E_{r_1}, a spatially uniform laser pulse carrying no information, precedes E_o, which carries the spatial information (e.g., an image) to be stored. The latter can be generated by transmission of a spatially uniform laser pulse through a spatial light modulator. The image thus recorded is a time-domain (or a spectral) hologram resulting from the interference of the temporally delayed pulses by interaction with dipoles in the storage material.[6,7]

The above recording procedure is repeated for subsequent images at different channels and can be initiated, for example, at the low-frequency side of the inhomogeneous line and completed at the opposite side by an incremental increase of the laser wavelength at the corresponding input rate. For an inhomogeneous bandwidth of 4 GHz (typical of a rare-earth solid) and $\Delta\nu = 1$ MHz, a total of 4000 images can be stored at one spatial location.

One recalls the image stored in a particular channel by tuning the laser wavelength to the channel location and exciting the sample with another reference pulse (or the read pulse, E_{r_2}), whose spatial profile is identical to that of E_{r_1}. The read pulse induces an echo that contains spatial information identical to that in E_o.[1,2]

The time required for recording a single frame, τ_s, is determined by the temporal widths of E_{r_1} and E_o and their separation. The last-mentioned parameter can be data-channel-width limited to maximize the recording speed (e.g., for a 1-MHz-wide data channel, the minimum separation can be as low as 1 μs). The channel switching time can be much shorter than

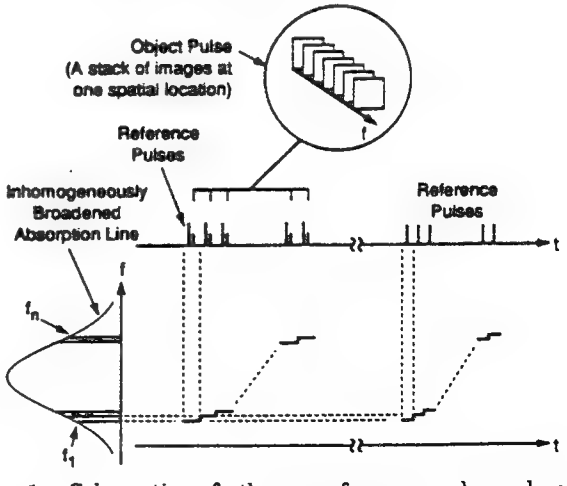

Fig. 1. Schematic of the one-frame-per-channel approach to image storage in CTDOM.

0146-9592/94/161246-03$6.00/0 © 1994 Optical Society of America

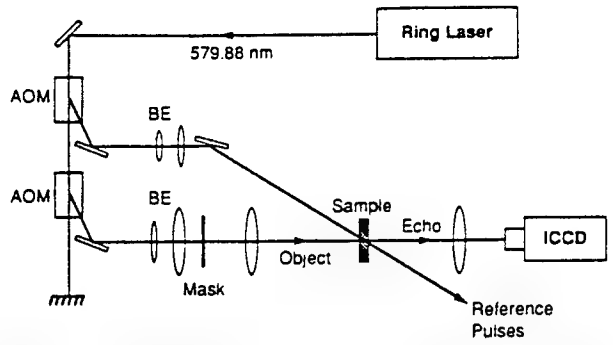

Fig. 2. Experimental setup for time-domain holographic image storage. AOM's, acousto-optic modulators; ICCD, intensified CCD camera; BE's, beam expanders.

τ_s for the small frequency increment proposed here (i.e., $\leq$1 MHz). Thus the upper limit of the recording speed is determined mainly by the reciprocal of τ_s, which can be estimated from the efficiency of a stimulated echo.

It is important to realize that the temporal profile of an echo does not have to be identical to its input in the proposed one-frame-per-channel approach. Thus the requirements on E_{r_1} and E_{r_2} can be relaxed considerably to permit the use of long reference pulses for efficient echo conversions with a low-power laser.

The efficiency of three-pulse echoes is found to be proportional to $\sin^2\theta_1 \sin^2\theta_2$ (here θ_i is the ith reference pulse area), with a maximum of ~0.5% (i.e., when $\theta_1 = \theta_2 = \pi/2$).[6,7] The efficiency is defined as the ratio of the echo intensity to the object beam intensity. For convenience, we assume that the laser used for image storage is a 500-mW single-frequency cw laser (commercially available) and that the images are reduced to approximately 1 mm × 1 mm before being stored in a CTDOM. Furthermore, the electronic transition used for image storage has a transition wavelength of 580 nm and an oscillator strength of $\sim 2 \times 10^{-6}$. Under this condition, the pulse area for a 1-μs-long square pulse is approximately equal to 1, giving rise to an echo efficiency of ~0.25%. If E_o is shorter than the reference pulses, the echo length is comparable with the length of the reference pulses.[7,8] To a good approximation, we can use the reference pulse length to estimate the total number of photons in an echo to be $\sim 4 \times 10^9$ (assuming that the object pulse power is also 500 mW). For a CCD camera consisting of 1000 × 1000 pixels, this gives an average intensity of ~4000 photons per pixel, a signal level strong enough for faithful retrieval.

The above estimate suggests that a cw laser of several hundreds of milliwatts is sufficient to store images in a CTDOM at megahertz rates. This feature of fast recording speed at a modest laser power is not to our knowledge available with other optical techniques for image storage, including accumulated photon echoes.[9]

Unlike conventional time-domain storage,[7] the one-frame-per-channel approach permits the playback speed to differ from the recording speed. The maximum playback speed is limited only by the length of E_{r_2} and thus can exceed the maximum recording speed, provided that the scattered light from read pulses in adjacent frequency channels does not interfere with the echo signal. Random frame access is now possible without further modification. Another advantage is that materials with short dephasing times ($\gtrsim\tau_s$) can be used here because of the short τ_s.

We have demonstrated experimentally the use of the proposed scheme for image storage in a Eu^{3+}:Y_2SiO_5 crystal (7 mm thick × 8 mm diameter and 0.1 at. %). The experiments were carried out on the $^7F_0$–$^5D_0$ transition (site 1 at 579.88 nm) of the crystal at ~2.5 K. This transition has an inhomogeneous linewidth of ~4 GHz, and its peak optical density for the sample is ~1.0. Figure 2 shows a schematic of the experimental arrangement. The reference and object pulses, of lengths 14 and 4 μs, respectively, were generated by modulation of a cw ring laser (Coherent Model 699-29, with a linewidth of $\leq$0.5 MHz) with two acousto-optic modulators. The object pulse was expanded to approximately 20 mm in diameter to illuminate masks for spatial encoding. The reference pulses were also expanded and collimated by a telescope, but only to ~2.5 mm. The peak power of the reference pulses (both E_{r_1} and E_{r_2}) was ~240 mW, and that of the object pulse was ~190 mW. For experimental convenience, the separation between E_{r_1} and E_o was chosen to be ~5 μs. Thus τ_s is 23 μs, giving rise to a recording speed of $\sim 4.3 \times 10^4$ frames/s.

The arrangement of E_o and E_{r_1} (E_{r_2}) was chosen to be similar to those used in conventional holographic data storage, i.e., E_o and E_{r_1} (E_{r_2}) propagate along different directions and intersect at the sample as shown in Fig. 2 (here the intersecting angle was ~6°). Instead of imaging the input on the sample to the size required for efficient echo generation, we used a single lens and placed it behind the mask to focus the image down to ~1 mm × 1 mm. An identical lens was used behind the sample to reconstruct the focused image back to its original form, which was then detected by a gated intensified CCD camera

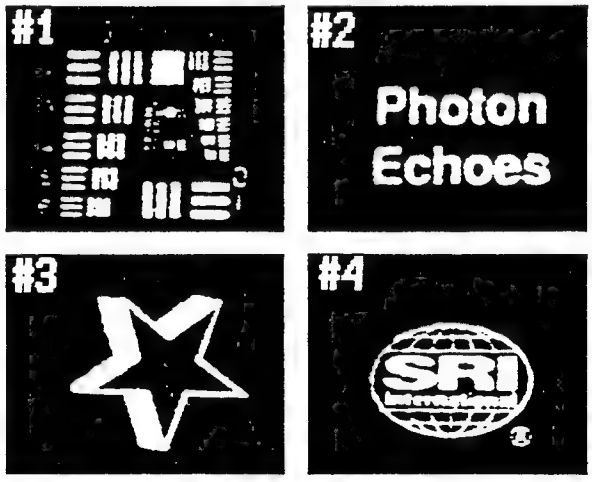

Fig. 3. Experimental results demonstrating the storage of multiple images in CTDOM. The label at the upper left corner of each image represents the data channel number. Each channel is 1 MHz wide and is separated from the next by 4 MHz. The images are recalled 5 min after the completion of the recording.

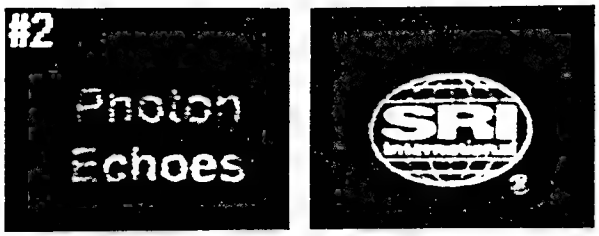

(a) (b)

Fig. 4. Echo images: (a) after repeated recall from data channel #2 14 times, (b) 2 h after the completion of the recording.

(a 6 mm × 4.5 mm CCD chip with 610 × 488 pixels). The separation between the mask and the focusing lens was chosen to be equal to the focal length. The image thus stored was only an approximate Fourier image (because the sample was not exactly in the focal plane), and, as a result, its dc terms were spread over a much larger area than that of an exact Fourier image to prevent image-dependent saturation at the center. This lens arrangement has several advantages. One can change the spot size of E_o at the sample continuously by adjusting the input lens position to achieve optimum intensity. The recalled images are less affected by small defects in the storage materials because any variation of material quality in the Fourier plane is distributed over the entire image on inverse transformation. Furthermore, storing Fourier images provides the memory with the ability to process the stored spatial information on retrieval, a unique feature that has been demonstrated elsewhere.[5]

Four images generated by different black-and-white transparencies were stored into four separate data channels by the proposed approach. The separation between two adjacent channels was chosen to be 4 MHz. The stored information was later recalled, and the results are shown in Fig. 3. The images were recalled 5 min after the completion of the recording, and they show no evidence of cross talk. In a separate experiment, the channel separation was reduced to 3 MHz, and again no cross talk was detected. The results here were obtained from single storage/retrieval events with no signal averaging, and the echo efficiency was measured to be $\sim 10^{-3}$.

In obtaining the above results, we biphase modulated the reference pulses (both E_{r_1} and E_{r_2}), using the 7-bit Barker code[10] to increase the data channel width to ~1 MHz. The purpose of this modulation was to prevent the data carrier frequency from drifting out of the channel during the recording.

The above stored images can be recalled repeatedly as many as 20 times, and the resulting echo images are still well within the detectable range of our recording system. Figure 4(a) shows such an example, which was obtained after repeated recall from the same data channel (channel #2) 14 times.

We further examined the effect of long storage times on the fidelity of the recalled images, an issue vitally important in practical applications. Currently such research can be carried out only on a time scale of several hours because of the lack of laser stability beyond this time scale. Figure 4(b) shows an image that was retrieved 2 h after the completion of the recording. Compared to Fig. 3, it shows no noticeable change in echo efficiency and fidelity, suggesting that a storage time of several days or longer may well be possible with this storage material.

The quality of the recorded echo images here was found to be limited by the nonuniform response of the gated image intensifier in the CCD camera, which varied from shot to shot. We compared the above images with their respective inputs detected by the same camera and found no measurable difference in image quality. We further recorded the same input images, using a conventional CCD camera having no microchannel-plate intensifier, and found a significant improvement in image quality. These findings suggest that the intrinsic quality of the images here is much higher than what was observed here.

In conclusion, we have proposed a new, practical scheme for storing images in CTDOM, which features random frame access and variable high recording/playback speeds. We have performed experiments to demonstrate its use for multiple image storage in Eu^{3+}:Y_2SiO_5. With a commercial cw ring laser, we have obtained an image recording speed of $\sim 4.3 \times 10^4$ frames/s, and the results show no evidence of cross talk between images that were stored less than 4 MHz apart.

This research was supported by the Advanced Research Projects Agency under contract F-49620-93-C-0076.

*Permanent address, Department of Physics, Massachusetts Institute of Technology, Cambridge, Massachusetts 02139.

References

1. N. W. Carlson, W. R. Babbitt, and T. W. Mossberg, Opt. Lett. **8**, 623 (1983).
2. M. K. Kim and R. Kachru, J. Opt. Soc. Am. B **4**, 305 (1987); Opt. Lett. **12**, 593 (1987).
3. B. Kohler, S. Bernet, A. Renn, and U. P. Wild, in *Persistent Spectral Hole-Burning: Science and Applications*, Vol. 16 of 1991 OSA Technical Digest Series (Optical Society of America, Washington, D.C., 1991), pp. 46–49; Opt. Lett. **18**, 2144 (1993).
4. F. H. Mok, M. C. Tackitt, and H. M. Stoll, Opt. Lett. **16**, 605 (1991); F. H. Mok, Opt. Lett. **18**, 915 (1993).
5. E. Y. Xu, S. Kröll, D. L. Huestis, R. Kachru, and M. K. Kim, Opt. Lett. **15**, 562 (1990); X. A. Shen and R. Kachru, Opt. Lett. **17**, 520 (1992).
6. I. D. Abella, N. A. Kurnit, and S. R. Hartmann, Phys. Rev. **141**, 391 (1966).
7. T. W. Mossberg, R. Kachru, S. R. Hartmann, and A. M. Flusberg, Phys. Rev. A **20**, 1976 (1979); T. W. Mossberg, Opt. Lett. **7**, 77 (1982).
8. Y. S. Bai, W. R. Babbitt, N. W. Carlson, and T. W. Mossberg, Appl. Phys. Lett. **45**, 714 (1984).
9. P. Saari, R. Kaarli, and A. Rebane, J. Opt. Soc. Am. B **3**, 527 (1986).
10. M. N. Cohen, in *Principles of Modern Radar*, J. L. Eaves and E. K. Reedy, eds. (Van Nostrand Reinhold, New York, 1987), p. 465.

Appendix C

HIGH SPEED STORAGE OF WAVELENGTH-MULTIPLEXED VOLUME SPECTRAL HOLOGRAMS

High Speed Storage of Wavelength-Multiplexed Volume Spectral Holograms

X. A. Shen, Y. S. Bai and R. Kachru
Molecular Physics Laboratory
SRI International
Menlo Park, CA 94025
Phone: (415) 859-3638; Fax: (415) 859-6196

ABSTRACT

We demonstrate a spectroholographic storage system for fast volume hologram recording. The achieved frame transfer rate exceeds 13 Kfps with random page access.

High Speed Storage of Wavelength-Multiplexed Volume Spectral Holograms

X. A. Shen, Y. S. Bai and R. Kachru
Molecular Physics Laboratory
SRI International
Menlo Park, CA 94025
Phone: (415) 859-3638; Fax: (415) 859-6196

One of the most attractive features of an optical memory is its ability to write and read data in a bit-parallel format, giving rise to theoretically very high (in excess of 1 Gbps) data transfer rates. However, such potential has not been demonstrated experimentally because of various inherent technical difficulties associated with existing optical storage techniques. In a photorefractive or a persistent spectral hole-burning (PSHB) memory, for example, the time required to record one page varies from a fraction of a second to several seconds.[1-3] For a page containing 1000×1000 bits of data, it translates to a bandwidth of approximately 1 Mbps, substantially slower than any existing semiconductor memories.

Coherent time domain optical memory (CTDOM) has shown potential for high speed data storage.[4-6] Fast recording and readout of sequential digital optical data in a CTDOM at 40 Mbps has been demonstrated,[4] and an I/O bandwidth of several Gbps is predicted for sequential recording. Recently, we proposed a practical scheme for parallel data storage in CTDOM. In a proof-of-principle experiment, four wavelength-multiplexed single-page volume spectral holograms, generated with black-and-white transparencies, were successfully stored in a single spatial location at a rate of approximately 43 Kfps. The results project an I/O bandwidth of the system to exceed 40 Gbps, which is 400 times faster than the bandwidth of a semiconductor cache memory.

Here we report on our scheme. a) to examine the feasibility of using a spatial light modulator (SLM) for information encoding in CTDOM (This work is needed because of the large insertion loss introduced by an SLM), b) to determine the realistic limit on recording speed of an SLM-based CTDOM, c) to examine the potential effect of wavelength multiplexing on diffraction efficiency as more holograms are stored. We successfully used wavelength multiplexing to record 100 spectral holograms at one spatial address in a $Eu^{3+}:Y_2SiO_5$ crystal. Despite the large insertion loss from the SLM, a frame recording speed in excess of 13 Kfps was obtained using a low power laser.

We performed our experiments on the $^7F_0$-$^5D_0$ transition (site 1 at 579.88 nm) of $Eu^{3+}:Y_2SiO_5$, which has an inhomogeneous linewidth of ~4 GHz and a dephasing time of ~1 ms. A computer entirely controlled recording and playback. In recording holograms, the computer first tuned to a desired wavelength (or data channel) within the inhomogeneously broaden absorption line, downloaded a preselected frame to an SLM through a frame grabber for information encoding, and then illuminated the sample with the reference and data pulses. We repeated this procedure at different channels until all 100 frames were stored. The data were later retrieved by illuminating each channel with a read pulse, and the reconstructed images were detected by a gated, intensified, CCD camera and digitized by the frame grabber.

The SLM used is a liquid crystal array taken from a projection television (InFocus TVT-6000). This array has 480 × 440 pixels and its insertion loss is approximately 97% for zero-order transmission. Two approaches can be used to compensate for the large loss: increase the laser power by a factor of 30, or increase the length of the data pulse since the camera detects time-integrated signals. The former approach is not practical because it would require a laser power of about 10 W. We chose the latter approach and used a 50 μs long data pulse with a peak power of only ~7 mW. The reference and read pulses were 14 μs long and biphase modulated with the 7-bit Barker code to obtain a data channel width of ~1 MHz. The separation between the reference and data pulses was 10 μs, which in principle, could be reduced to ~1 μs to increase the recording speed. The recording speed was 74 μs/frame, or 13.5 Kfps. Further details about the experiments are given elsewhere.[5]

Five minutes after the recording was completed, we read out the data by illuminating each spectral grating with the read pulse. Figure 1 shows some of the reconstructed images. The 100 stored images were spaced evenly across a spectral window that was ~300 MHz wide and occupies only 7.5% of the inhomogeneous linewidth. Under this condition, we saw neither cross talk nor any effect on diffraction efficiency. A nearly constant efficiency of ~10^{-3} was measured.

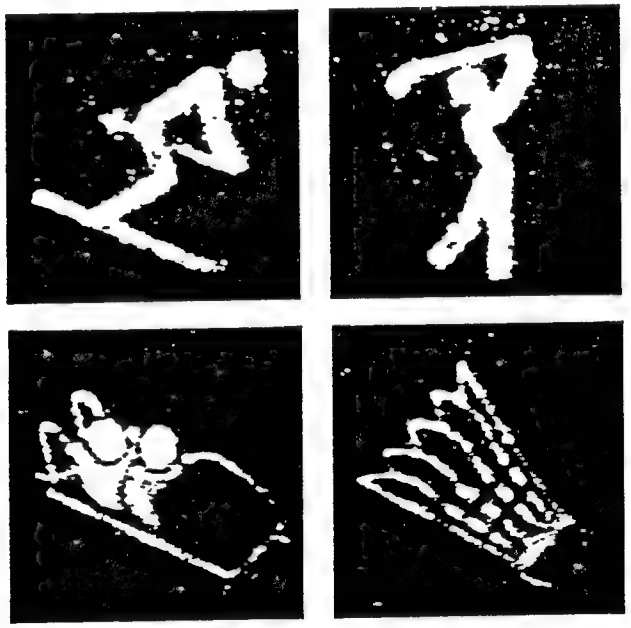

Fig. 1. Experimental results showing 4 out of 100 reconstructed spectral holograms.

Because there are two distinct optical sites for the $^7F_0$-$^5D_0$ in Eu^{3+}:Y_2SiO_5,[7] our results suggest a minimum storage capacity of 2660 frames per spatial spot (or 1330 frames per optical site) for this one-frame-per-channel approach. We believe that by reducing the data channel width to ~0.5 MHz with a frequency-stabilized laser, a capacity of over 4000 frames per spatial spot is achievable in Eu^{3+}:Y_2SiO_5. We can further estimate this capacity for binary digital data storage. Assume that each page has 1000 × 1000 pixels and each information bit is represented by a block of 4 × 4 pixels. Under this condition, one would obtain a capacity in excess of 250

Mbits per spot. By taking into account the spot size (which is ~$1.0 \times 1.0 \times 7.0$ mm),[5] we would have a density of ~35 Gb/cm^3.

The above estimate can be further extended to the system's I/O bandwidth. For a page containing 250×250 bits, the achievable data throughput rate would exceed 840 Mbps. A more optimistic estimate that assumes one bit per pixel would yield a bandwidth of over 10 Gbps, which is 100 times faster than the existing semiconductor cache memory.

In conclusion, we demonstrated the storage of 100 single-page spectral holograms at a single spatial location in a Eu^{3+}:Y_2SiO_5-based CTDOM using an SLM. The large insertion loss introduced by the SLM has no significant effect on system performance. A frame transfer speed of more than 1.3 Kfps was obtained with a modest laser power. Experiments to demonstrate the storage of a much larger number of holograms are underway to fully utilize the entire inhomogeneously broadened absorption line.

References

1. F. H. Mok, M.C. Tackitt, and H. M. Stoll, Opt. Lett. **16**, 605 (1991); F. H. Mok, Opt. Lett. **18**, 951 (1993).
2. B. Kohler, S. Bernet, A. Renn, and U. P. Wild, Opt. Lett. **18**, 2144 (1993).
3. J. F. Heanue, M. C. Bashaw, and L. Hesselink, Science **265**, 749 (1994).
4. Y. S. Bai and R. Kachru, Opt. Lett. **18**, 1189 (1993).
5. X. A. Shen, E. Chiang, and R. Kachru, Opt. Lett. **19**, 1246 (1994).
6. T. W. Mossberg, Opt. Lett. **7**, 77 (1982).
7. R. Yano, M. Misunaga, and N. Uesugi, Opt. Lett. **16**, 1884 (1991).

Appendix D

OPTICAL HEADER RECOGNITION BY SPECTROHOLOGRAPHIC FILTERING

Optical header recognition by spectroholographic filtering

X. A. Shen and R. Kachru

Molecular Physics Laboratory, SRI International, Menlo Park, California 94025

Received June 9, 1995

We report on a novel scheme based on spectral holography for high-speed processing of optical header information. In this scheme, we rapidly analyze each incoming header by performing simultaneous correlation operations with a large number of headers stored in advance through angular multiplexing. Decoding is accomplished by identification of the directions that yield the maximum correlation signal. In a proof-of-concept experiment, two 5-byte ASCII addresses were decoded successfully without any ambiguity. The potential of this technique for high-speed packet switching is discussed. © 1995 Optical Society of America

Packet switching has emerged as a promising networking technique capable of supporting a wide range of communications services, such as voice, video, image, and data.[1,2] However, implementation of this technique at optical carrier frequencies for full utilization of the wide transmission bandwidth offered by fiber-optic technologies remains a challenge. One of the impediments to the development of this technique is its inability to permit rapid analysis of temporal optical information contained in the header of each packet for efficient routing. Most existing optical processors[3,4] suffer from either insufficient memory capacity for storing reference information or slow processing speed for routing at required packet rates.

In this Letter we propose and demonstrate a novel scheme for rapid processing of temporal optical signals, such as optical headers. This scheme utilizes simultaneously three attractive features offered by the time-domain optical memory[5-12] (TDOM): the ability to perform in-memory temporal signal processing, high capacity for sequential data storage, and the ability to store reference signals through angular multiplexing. Combination of these three features permits TDOM to simultaneously compare an incoming header and a large number of reference headers stored in advance through angular multiplexing for rapid parallel header processing, increasing significantly the processing speed.

The proposed scheme is illustrated schematically in Fig. 1. In the programming phase, reference headers to be used for analysis are first stored in TDOM at one spatial location by their respective brief write pulses through angular multiplexing. The reference headers (later the unknown headers to be analyzed) are chosen to propagate along a common direction $\hat{k}$ and are angularly multiplexed by variation of only the incident angle of the write pulses, e.g., the ith reference header H_i is stored by the ith write pulse W_i propagating along $\hat{k}_i$. This process stores not only H_i for subsequent processing but also the propagation direction $\hat{k}_i$.

In TDOM, stored data are retrieved by use of a read pulse.[5] The pulse induces coherent radiation (often referred to as echoes) that mimics the temporal data sequence originally stored. Unlike other memory devices, data retrieval in TDOM is actually a process of temporal signal processing. In the case when a brief write pulse is used, the retrieved information represents either correlation or convolution of the read pulse with the stored data, depending on the order in which the write pulse is used.[6] With the choice of the pulse pair shown in Fig. 1, the processing is simply a correlation operation, and the resulting echo is known to emit along the same direction as that of the write pulse. Thus, in order for the retrieved information to be identical to the stored information, a brief read pulse must be used. (Note that correlation of any function with a delta pulse yields the function itself.)

Parallel header decoding can now be realized as follows. If, instead of a brief read pulse, an unknown header H (propagating along $\hat{k}$) arrives at the sample at a later time, the echo generated along $\hat{k}_i$ is the correlation of H with H_i. A large correlation peak occurs when a match to H_i is found (i.e., $H = H_i$). Thus one can identify H by examining the intensities of the correlation peaks along each direction.

The advantage of monitoring correlation peaks is that decisions can be made very rapidly. The peaks

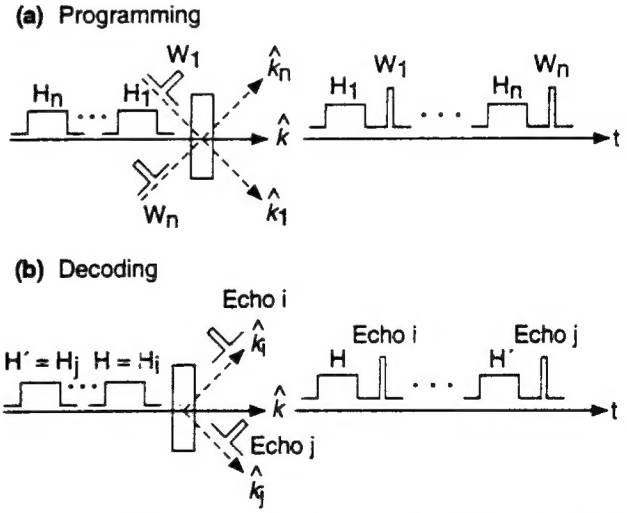

Fig. 1. Schematic of the proposed scheme for optical header decoding. (a) The storage material is first programmed by exposure to n successive pulse pairs, each of which contains a reference header H_i and a write pulse W_i; each W_i is chosen to propagate along a different direction $\hat{k}_i$. (b) During the decoding, the sample is reexposed to unknown headers, and the echoes emitting in different directions are detected and compared.

0146-9592/95/242508-03$6.00/0 © 1995 Optical Society of America

can be chosen to occur immediately after the arrival of an unknown header by minimization of the separation between the last data bit of H_i and W_i in the programming phase. This separation is limited only by the bandwidth of data contained in H_i. For a bandwidth of 1 GHz, the separation can be as small as 1 ns. Thus the correlation peaks appear only 1 ns after the arrival of an unknown header.

It is clear that once a header is decoded in packet switching, information following the header is routed at the *packet* rate rather than the data rate. Thus no additional bandwidth is needed for routing, unlike in other routing schemes such as the one proposed by Babbitt and Mossberg.[7] In their approach, each data bit is routed individually by phase encoding, resulting in a switching bandwidth much larger than the data bandwidth.

In a proof-of-concept experiment, we have successfully decoded two 5-byte optical headers by using the proposed scheme. For the purpose of demonstration, we chose the intensities of the two headers to represent the zip codes of SRI International and the Advanced Research Projects Agency in binary ASCII (i.e., 94025 and 22203, respectively). However, use of entirely amplitude-modulated headers would lead to ambiguities in header decoding unless additional bits were employed to suppress peaks from cross correlations (i.e., $H \neq H_i$). Such an approach would reduce the processing speed significantly and is not desirable. We introduce interpulse biphase modulation to suppress cross-correlation peaks. In addition to being amplitude modulated, each header is further encoded according to a unique predetermined pseudorandom biphase code (i.e., the phase of each data bit was randomly selected to be either positive or negative). This interpulse phase modualtion is easy to implement and does not require the use of extra data bandwidth. Most importantly, it effectively suppresses not only the cross-correlation peaks but also sidelobes obtained from either autocorrelation or cross correlation, permitting clear header identifications.

The apparatus used in the present experiment is similar to that reported in Ref. 13. One major modification to our early apparatus is the replacement of a commercial ring dye laser with a frequency-stabilized laser (a modified Coherent 699-29 ring dye laser). This laser was locked to an external cavity by the Pound–Drever–Hall scheme[14] with the aid of an intracavity electro-optic modulator (Gsänger PM 25). The laser linewidth with respect to the external cavity was measured to be approximately 40 kHz.

To generate two zip codes and their respective write pulses as shown in Fig. 1, we employed three acousto-optic modulators and placed them in serial in the beam pass, each of which was used in a double-pass configuration. One acousto-optic modulator was responsible for generating two biphase-encoded zip codes, and the other two were responsible for generating two brief (~150-ns-long) write pulses in two separate directions. The experiment was carried out on the $^7F_0$–$^5D_0$ transition (Site 1 at 579.88 nm) of an ~0.1 at. % Eu^{3+}:Y_2SiO_5 crystal (7 mm thick × 8 mm diameter) at ~2.5 K. The three beams (one header beam and two write beams) were made to converge at the sample at a crossing angle of ~30 mrad by a focusing lens, resulting in a focal spot (FWHM) at the sample of ~25 μm. The laser was operated at a wavelength that produced a linear absorption by the sample of approximately 55%. The peak power of the write pulses was chosen to be ~100 mW. The intensity of the headers was reduced to a value approximately a factor of 20 smaller than that of the write pulses.

Figure 2 shows the experimental results. We first stored zip code 94025 by using a write pulse propagating along $\hat{k}_1$; 12 μs later, zip code 22203 was stored by another write pulse propagating along $\hat{k}_2$. Each "on" bit in the headers was represented by a 150-ns laser pulse, and the length of the headers was 12 μs. For experimental convenience, we chose the separation between the header and the write pulse in each pulse pair to be 12 μs. As discussed above, this separation can be reduced to 150 ns for the modulation used here.

After the completion of the header storage, we reexposed the sample first to zip code 94025 and then to zip code 22203 for decoding. The resulting correlation signals emitting in directions $\hat{k}_1$ and $\hat{k}_2$ were detected by two photodetectors. We chose the time between the completion of the memory programming and the

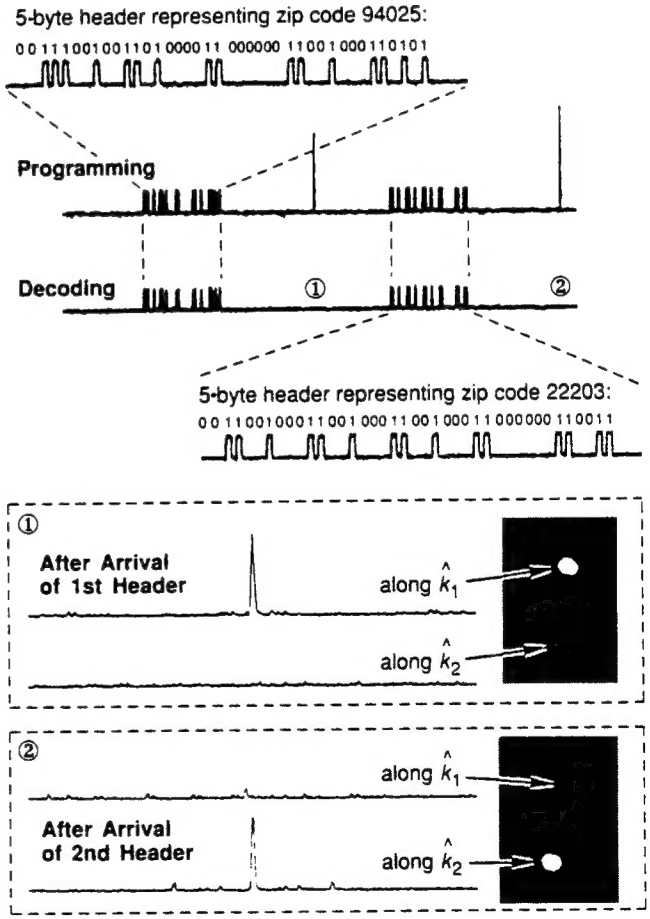

Fig. 2. Experimental results showing the successful decoding of two zip codes. The second and third traces from the top display the input pulse sequence; the first and fourth traces are the two input zip codes on an expanded time scale. The recorded correlation signals along $\hat{k}_1$ and $\hat{k}_2$ after the arrival of zip code 94025 and zip code 22203 are shown in boxes 1 and 2, respectively.

start of the header decoding to be ~11 ms, much longer than the excited-state lifetime of the $^7F_0-^5D_0$ transition (i.e., 2 ms).[15] It is known that the reference information used under such a condition in $Eu^{3+}:Y_2SiO_5$ can persist for hours or longer.[11,13] Box 1 in Fig. 2 shows the correlation signal along $\hat{k}_1$ and $\hat{k}_2$ after the arrival of zip code 94025. We obtained a strong correlation peak along $\hat{k}_1$ and no measurable peak along $\hat{k}_2$, indicating a good match to zip code 94025 and no match to zip code 22203. After the arrival of zip code 22203 (i.e., 24 μs later), the situation is reversed (see box 2 in Fig. 2). No match was found along $\hat{k}_1$, whereas a good match was found along $\hat{k}_2$. As expected, the detected sharp peaks occurred exactly 12 μs after the arrival of each zip code (recall that the separation between H_i and W_i is 12 μs). Here, each correlation trace is 20 μs long and was recorded from a single processing event with no signal averaging.

We further demonstrated this parallel decoding of zip codes by using a CCD camera to resolve the correlation peaks spatially and temporally. Since these peaks occurred in a well-defined time interval, we gated the camera with a 200-ns pulse to detect the peaks only. The results (also shown in Fig. 2) are in good agreement with the time-resolved measurements.

We repeated the above experiment in the absence of the interpulse phase modulation and obtained, in addition to large sidelobes of various amplitudes, a cross-correlation peak that was only 50% smaller than the autocorrelation peaks. Comparison with Fig. 2 clearly shows the effectiveness of the phase modulation in suppressing large undesirable signals from both autocorrelations and cross correlations. We point out that the time-resolved measurements presented in Fig. 2, along with those obtained without the use of the biphase modulation, have been carefully compared with calculations, and the agreement was excellent.

The proposed scheme can be readily used to decode headers containing multiple fields (e.g., in asynchronous transfer mode switching, each 5-byte header has, in addition to address, information about data type and priority, etc.). To do so, one must treat each field as a separate header and store them individually using the same approach described above. The memory thus programmed would direct correlation results for each field into a separate spatial location for individual identifications.

In conclusion, we have proposed a novel scheme for parallel processing of large-bandwidth temporal optical signals. We have further applied this scheme to header recognition in packet switching to decode two 5-byte addresses successfully. Headers containing multiple fields can also be processed with minor modifications. The ability to decode optical headers, along with the demonstrated high capacity for large-bandwidth optical data storage, opens up the possibility of using TDOM for high-speed optical packet switching with features such as self-routing and large optical buffers.

This research was supported by the Advanced Research Projects Agency under contract F-49620-93-C-0076.

References

1. F. A. Tobagi, IEEE **78,** 133 (1990).
2. T. F. La Porta, M. Veeraraghavan, E. Ayanoglu, M. Karol, and R. D. Gitlin, IEEE Commun. Mag. (October 1994), p. 84, and references therein.
3. K. P. Jackson and H. J. Shaw, in *Optical Signal Processing*, J. L. Horner, ed. (Academic, New York, 1987), and references therein.
4. N. J. Bers, J. L. Lee, M. W. Casseday, and B. J. Udelson, Appl. Opt. **18,** 2767 (1979), and references therein.
5. T. W. Mossberg, Opt. Lett. **7,** 77 (1982).
6. Y. S. Bai, W. R. Babbitt, N. W. Carlson, and T. W. Mossberg, Appl. Phys. Lett. **45,** 714 (1984); Y. S. Bai, W. R. Babbitt, and T. W. Mossberg, Opt. Lett. **11,** 724 (1986).
7. W. R. Babbitt and T. W. Mossberg, Opt. Lett. **20,** 910 (1995).
8. S. Kröll, L. E. Jusinski, and R. Kachru, Opt. Lett. **16,** 517 (1991).
9. M. Mitsunaga, M. K. Kim, and R. Kachru, Opt. Lett. **13,** 536 (1988).
10. X. A. Shen, Y. S. Bai, E. M. Pearson, and R. Kachru, U.S. patent 5,381,362 (January 11, 1995); X. A. Shen, Y. S. Bai, and R. Kachru, Opt. Lett. **17,** 1079 (1992).
11. Y. S. Bai and R. Kachru, U.S. patent 5,369,665 (November 29, 1994).
12. M. Mitsunaga, R. Yano, and N. Uesugi, Opt. Lett. **16,** 1890 (1991).
13. X. A. Shen, E. Chiang, and R. Kachru, Opt. Lett. **19,** 1246 (1994).
14. R. W. P. Drever, J. L. Hall, F. V. Kowalski, J. Hough, G. M. Ford, A. J. Munley, and H. Ward, Appl. Phys. B **31,** 97 (1983).
15. R. Yano, M. Mitsunaga, and N. Uesugi, Opt. Lett. **16,** 1884 (1991).